Brookhaven National Laboratory Report

BNL-NUREG-34790 (1984)

IMMERSION TEST AND SURFACE STUDIES FOR CREVICE CORROSION OF GRADE-12 TITANIUM IN A BRINE SOLUTION AT 150°C

T. M. Ahn, R. Sabatini* and P. Soo

Department of Nuclear Energy
Brookhaven National Laboratory
Upton, New York 11973

*Department of Applied Science
Brookhaven National Laboratory
Upton, New York 11973

Key Description: Titanium, Crevice Corrosion, Surface Studies, Immersion Test

ABSTRACT

The crevice corrosion behavior of ASTM Grade-12 titanium (Ti-0.3 Mo-0.8 Ni) was investigated in simulated rock salt brine solutions at a temperature of 150°C. A distinct corrosion product with a range of interference colors was observed in a mechanically simulated crevice after two to four weeks' exposure. Low pH (~4) accelerated the reaction rate and deaerated solutions gave less voluminous corrosion than aerated ones. Also, increasing specimen size, decreasing crevice gap, and preoxidation of the cathodic area gave more crevice attack. Higher temperatures (~250°C) do not necessarily accelerate crevice corrosion. These results are consistent with those expected from macroscopic concentration cell formation accompanied by oxygen depletion, potential drop, and acidification inside the crevice. TEM and SEM techniques were extensively utilized to identify the structure of the film formed inside the crevice at each stage of the corrosion process. In the early stage of cell formation, anatase-type TiO_2 was formed which acted as a barrier to further corrosion inside the crevice. In the case of severe crevice corrosion, which was accompanied by pitting, the corrosion product was identified as the rutile form of TiO_2 which is not an effective barrier to further corrosion. EDAX, Auger and Rutherford Backscattering spectra showed Ni depletion in the crevice corrosion products, while Mo was depleted on the top surface of the corrosion products and it was enriched in the interior of the corrosion products. This is consistent with the anticipated behavior of dissolved Ni and Mo ions. Based on the data for the structure and chemistry of oxides formed in the crevice, a new mechanism is proposed for the crevice

corrosion of Grade -12 titanium in simulated rock salt brines. It is believed that, initially, compact anatase crystals are formed inside the crevice. As the macroscopic cell develops, the beta phase, enriched with Mo and Ni, reaches the transpassive pitting potential resulting in localized dissolution. During the localized dissolution, rutile crystals are formed in the crevice.

FIGURES

FIGURES (Continued)

TABLES

1. INTRODUCTION

There is currently in the U.S.A. an effort to develop titanium alloy ASTM Grade-12 (Ti - 0.3 Mo - 0.8 Ni) as a candidate corrosion resistant material for high level nuclear waste containers which will be emplaced in mined geologic repositories such as those in rock salt [1-7]. Crevice-type environments are expected to form between the Grade-12 titanium container and surrounding backfill materials or metallic emplacement sleeves. Earlier screening tests of various candidate materials showed that Grade-12 titanium is immune to crevice corrosion in simulated rock salt brines (neutral pH) below 300°C and dissolved oxygen concentrations below 250 ppm [1]. This immunity has been attributed to the addition of Mo and Ni to titanium [8] since pure titanium shows significant crevice corrosion in neutral brines between approximately 100-150°C [9,10]. Although the crevice corrosion of Grade 2 (commercially pure) and Grade 7 (0.12 ~0.25 weight percent Pd alloy) titanium has been studied to a certain extent [9-13], no detailed information on the corrosion mechanism is available in Grade-12 or other titanium alloys. This first paper outlines the results of immersion tests and surface analysis studies on Grade 12 titanium. The main objectives were to determine whether crevice corrosion is likely in Grade-12 titanium when exposed to simulated rock salt brines at 150°C and to ascertain the probable mechanisms involved. In the immersion test, we emphasize the effects of solution chemistry, such as oxygen and proton concentrations, and the effects of sample geometry. The composition and structure of oxide formed were identified to understand the initial stage of crevice corrosion and the role of alloying elements. The next two papers in this journal will summarize the results of electrochemical

studies and mass balance calculations and these will quantify and support the corrosion mechanism proposed here.

2. MATERIALS AND TEST ENVIRONMENTS

Grade-12 titanium is a two-phase material composed of alpha phase and about ten volume percent beta phase along grain boundaries, as shown in Figure 1. Sheet materials used in the study were obtained from TIMET Corporation. The vendor supplied composition is shown in Table 1. Ni, Mo and Fe tend to concentrate in the beta phase and to dilute in the alpha phase. In the beta phase, up to 4.3 weight percent Ni and 1.3 weight percent Mo were detected using an EDAX* probe. No more than 0.30 weight percent Ni and no Mo were detected in the alpha phase. The differences in Fe concentration were relatively small compared to those for Mo and Ni.

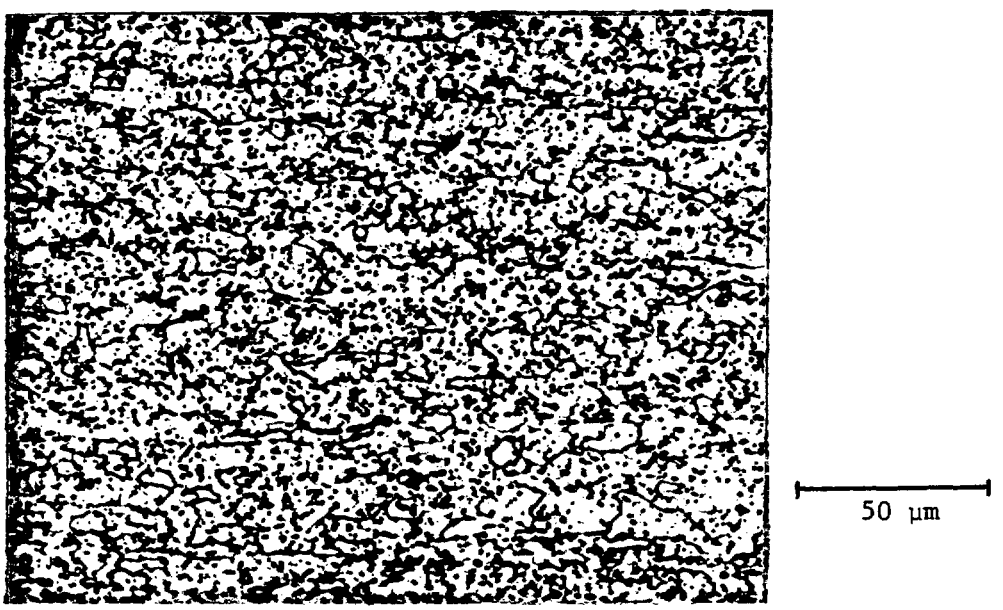

Figure 1. Initial microstructure of Grade-12 Titanium.

*EDAX is a commercial name for the procedure of Energy Dispersive Analysis of X-rays.

Table 1. Compositions of ASTM Grade-12 titanium supplied by vendor (weight percent).

Ni	Mo	Fe	C	H	N	O	Ti
0.82	0.29	0.09	0.013	0.01	0.15	0.16	Balance

Brine solutions selected for this study were based on those used by Sandia National Laboratories (1) which are considered to simulate those at the Waste Isolation Pilot Plant site in New Mexico. The concentrations of the major ions in the solutions used are shown in Table 2. The solutions are nearly saturated with Cl^-, K^+, Na^+, and Mg^{+2} (Brine A) ions or Cl^- and Na^+ (Brine B) ions. The initial pH values of the solutions are near neutral. The majority of the work was performed with Brine A, and the main test temperature was 150°C.

Table 2. Compositions of brine solutions (ppm).

Brine	Na^+	K^+	Mg^{+2}	Ca^{+2}	Sr^{+2}	Cl^-	SO_4^{-2}	I^-	HCO_3^-	Br^-	BO_3^-	pH
A	42000	30000	35000	600	5	190000	3500	10	700	400	1200	6.5
B	115000	15	10	900	15	175000	3500	10	10	400	10	6.5

3. EXPERIMENTAL PROCEDURES

Three different sizes of coupon were used (1 x 2, 2 x 2, and 2 x 4 cm) for the tests. After mirror polishing of the coupons up to 6 μm diamond paste, a crevice was made by joining metal/metal or metal/Teflon couples with titanium bolts. The bolts were insulated from the sample in later tests. However, it was found that the presence of insulated bolts gave no significant difference in the results obtained.

The immersion studies were performed in quartz tubes or in static autoclaves for two to four week periods. The acidity and oxygen concentration of the solutions were varied and the degree of corrosion was examined optically. Figure 2 shows a specimen which was bent to detach the thick oxide scale formed during severe attack. To identify the oxide, a sample from inside the crevice was selected by punching out from the coupon an area of diameter 3.2 mm. The punched area was carbon coated and the oxide was stripped off chemically by the immersion of the punched area in a 2% HF solution. HF dissolves the titanium substrate [14] but does not attack the oxide itself in a few minutes [15. 16]. The scale was identified by TEM electron diffraction analysis. The precise composition of the oxide formed was also analyzed by EDAX

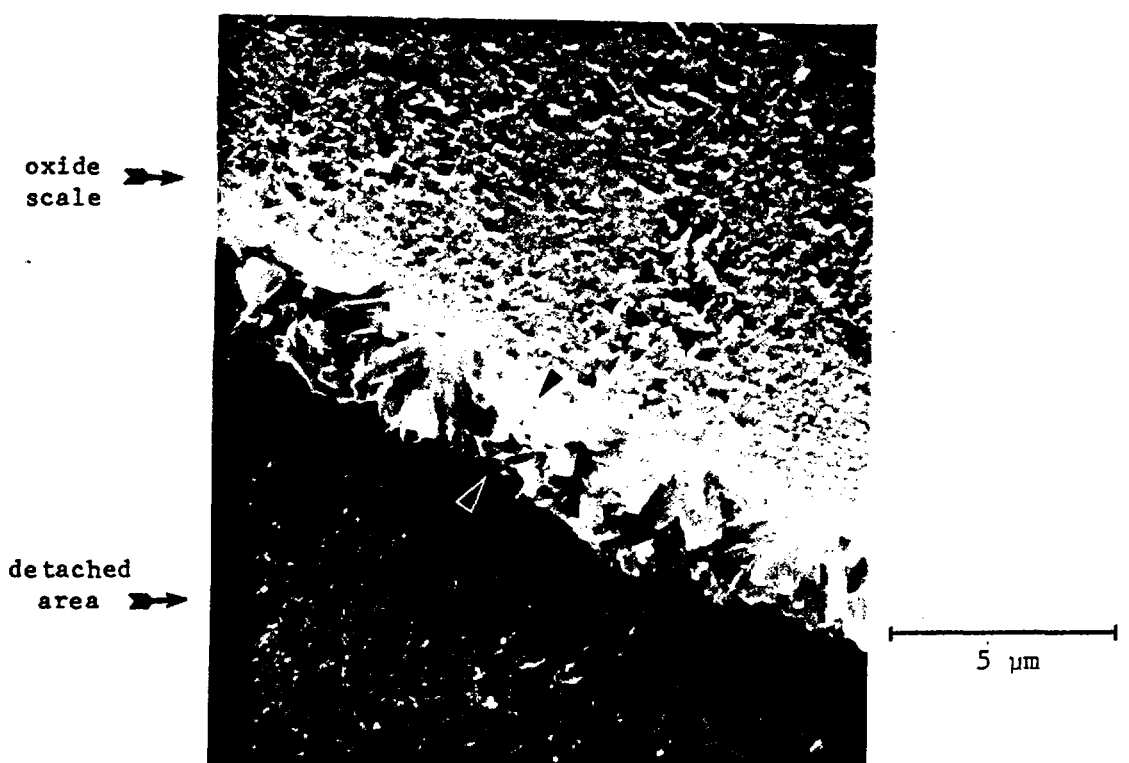

Figure 2. Detached oxide inside a Grade-12 titanium crevice after six weeks' exposure in aerated Brine A at 150°C. Arrow indicates the thickness of oxide.

probe. Prior to the EDAX probe measurements, the sample was mounted in epoxy to reveal the cross section of the sample preserving the oxide adhered (Figure 3). The EDAX results were confirmed by Rutherford Backscattering and Auger Spectroscopic Analysis of which procedures are described elsewhere (see Acknowledgment).

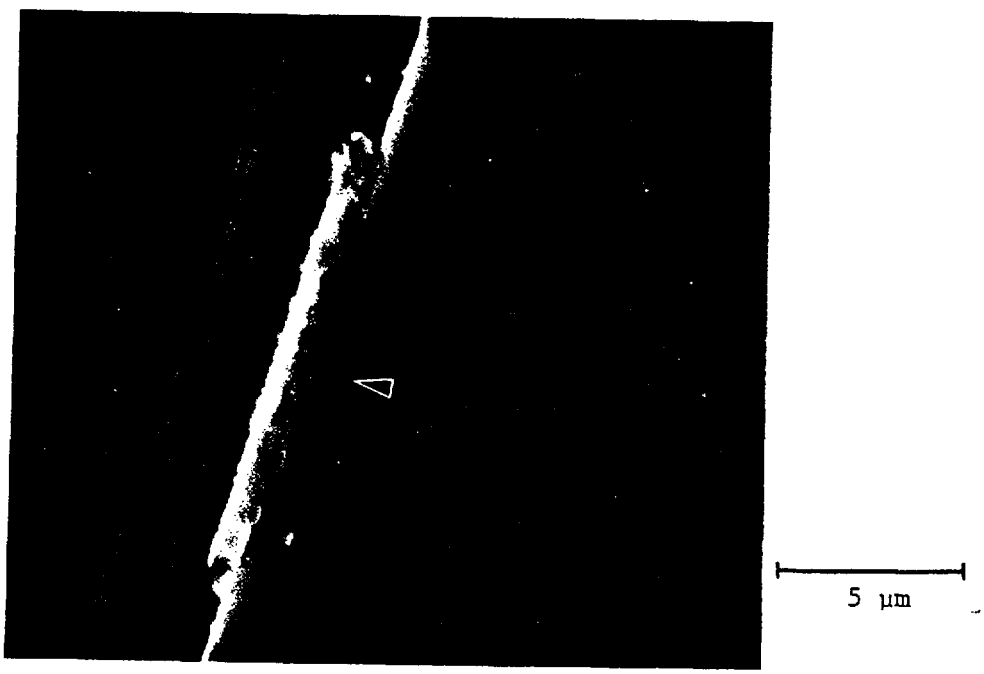

Figure 3. Intact oxide used for chemical analysis by EDAX (arrow mark). The oxide was obtained from a Grade-12 titanium crevice after six weeks' exposure in aerated Brine A at 150°C.

4. RESULTS

During the initial stage of crevice corrosion (first few days of immersion), a very thin multicolored corrosion product was observed. This type of film was more common in smaller samples, and remained for exposures greater than two weeks. Three distinct concentric areas (blue, violet, and yellow)

were selected for electron diffraction. Regardless of the color, the diffraction patterns showed strong anatase TiO_2 peaks with traces of Ti_3O_5 also present. A typical diffraction pattern is shown in Figure 4. The anatase form of TiO_2 was mostly present as block-shaped crystals as shown in Figures 5 and 6. For exposures of over two weeks, the largest samples (2 x 4 cm) with the smaller crevice gaps (metal/Teflon) showed a major black corrosion product. This was composed of the rutile form of TiO_2 as identified from the diffraction pattern in Figure 7. The rutile was in the form of needle-shaped crystals as shown in Figures 8 and 9.

A typical example of severe attack is shown in Figure 10. The degree of attack is determined using the SEM as shown in Figure 1. A type of pitting is often observed in such severely attacked specimens as shown in Figure 11.

A supplementary series of tests led to the following conclusions:

(a) Aerated solutions caused more severe attack than deaerated ones

(b) Aeration with pure oxygen gave more corrosion than aeration with air

(c) Preoxidation of cathodic parts of the specimen in air enhanced crevice attack

(d) Lower pH brine (~4 to 5) enhanced crevice attack

(e) Increasing the test temperature to 250°C gave less crevice attack compared to tests conducted at 150°C.

Table 3 shows the EDAX analysis of the crevice corrosion products. They are shown to be enriched in Mo and depleted in Ni, compared to the starting material. However, the Auger spectrum and the Rutherford Backscattering spectrum did not detect these two elements (Figures 12 and 13).

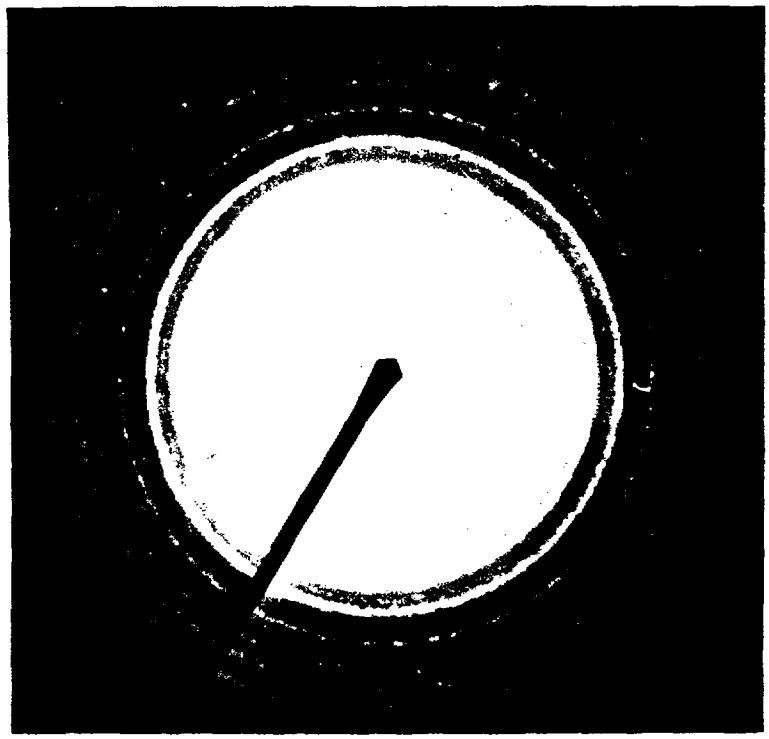

Figure 4. Typical diffraction pattern of anatase in an ASTM Grade-12 titanium crevice. A lower oxide peak is also noticeable. The film was selected from a sample which was immersed in Brine A at 150°C for four weeks.

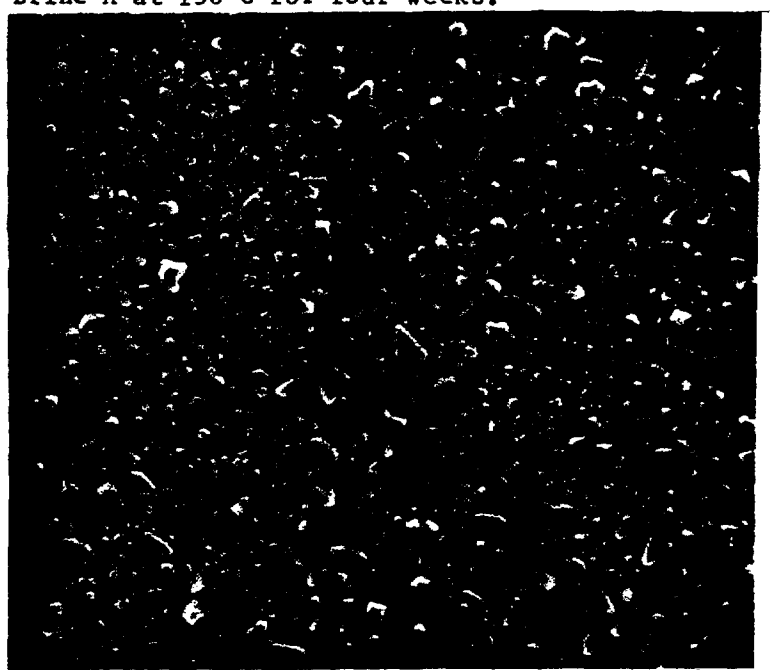

Figure 5. Typical SEM micrograph of the anatase form of TiO_2 formed during the initial stage of crevice corrosion in Brine A exposed for two weeks at 150°C.

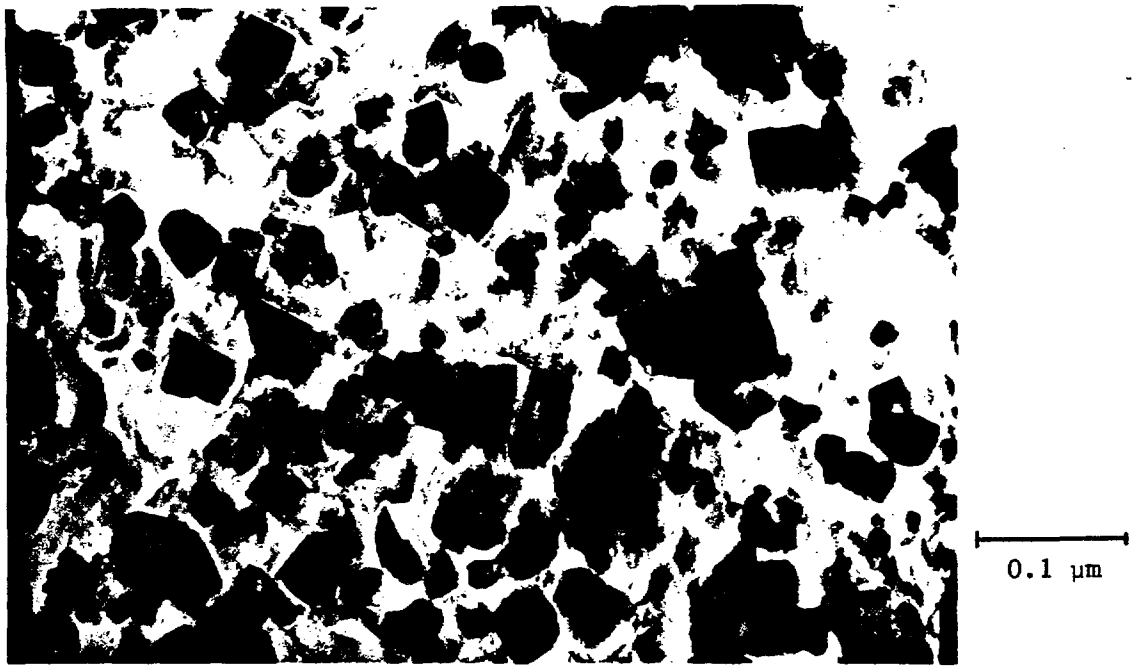

Figure 6. Typical TEM micrograph of the anatase form of TiO_2 formed during the initial stage of crevice corrosion in Brine A exposed for two weeks at 150°C.

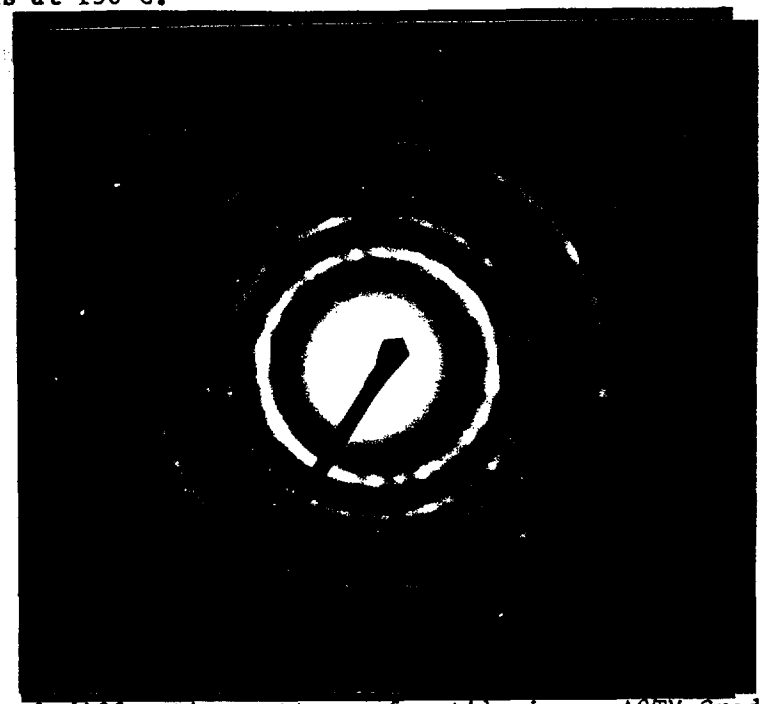

Figure 7. Typical diffraction pattern of rutile in an ASTM Grade-12 titanium crevice. The film was selected from a black oxide area in a sample which was immersed in Brine A at 150°C for two weeks.

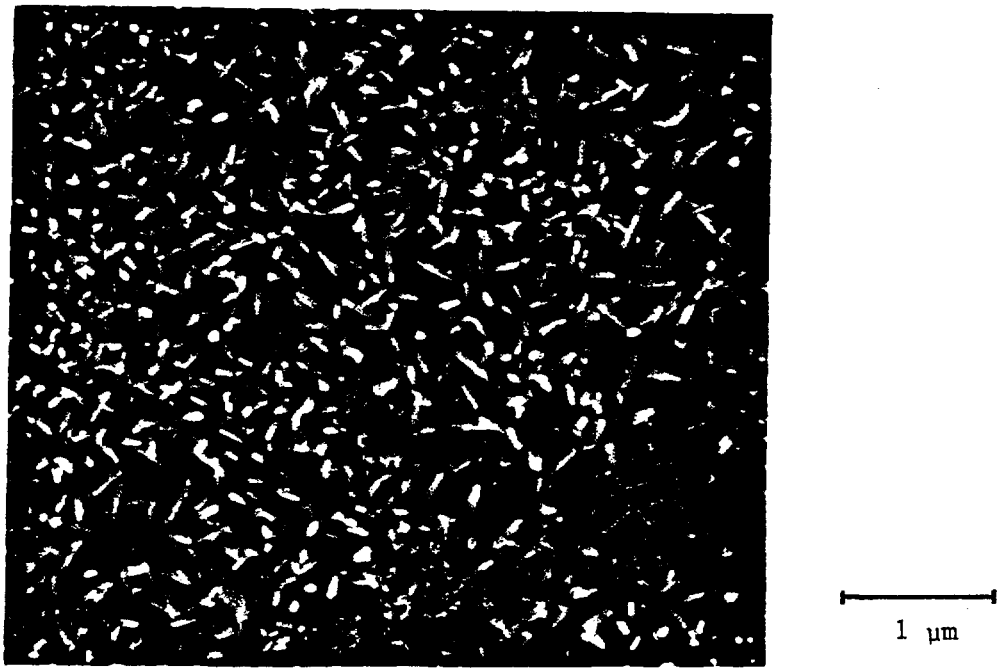

Figure 8. Typical SEM micrograph of the rutile form of TiO_2 formed during crevice corrosion in Brine A for two to four weeks at 150°C.

Figure 9. Typical TEM micrograph of the rutile form of TiO_2 formed during crevice corrosion in Brine A for two to four weeks at 150°C.

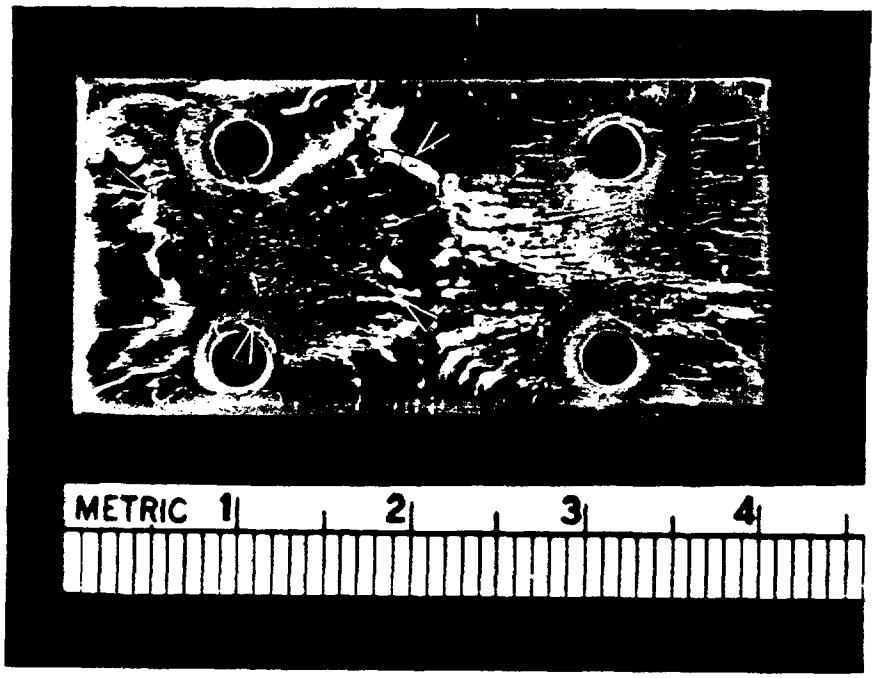

Severe attack

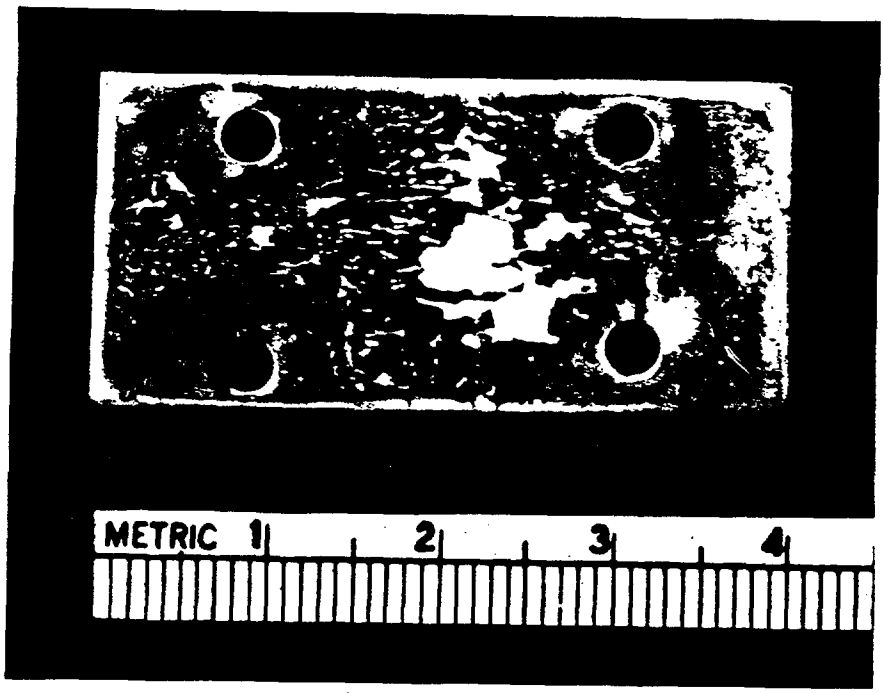

Initial stage of attack

Figure 10. Optical micrographs of severe crevice corrosion and the initial stage of attack in oxygenated and deoxygenated Brine A, respectively, after two weeks at 150°C. The arrow shows the black rutile form of TiO_2.

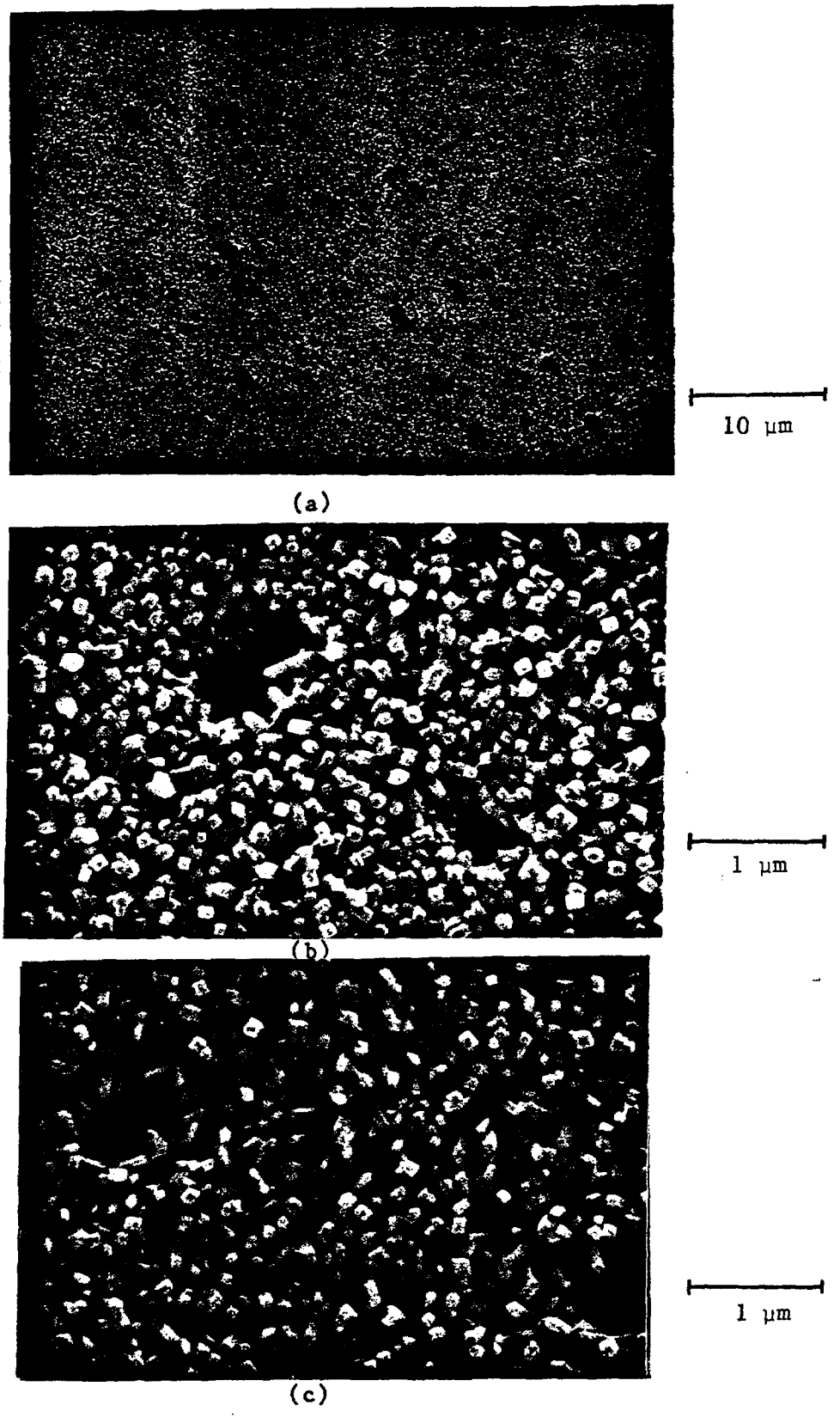

Figure 11. Pit-type morphology in rutile crystals from an ASTM Grade-12 crevice sample exposed for six weeks in oxygenated Brine A at 150°C.

Table 3. EDAX analysis results on the corrosion products in a crevice exposed to oxygenated Brine A for two weeks at 150°C. (Weight percent.)

Element	As-Received Sample	Crevice Corrosion Products
Mo	0.29-0.30	0.53
Ni	0.74-0.82	0.07
Fe	0.09	0.07
Balance	Ti	TiO_2

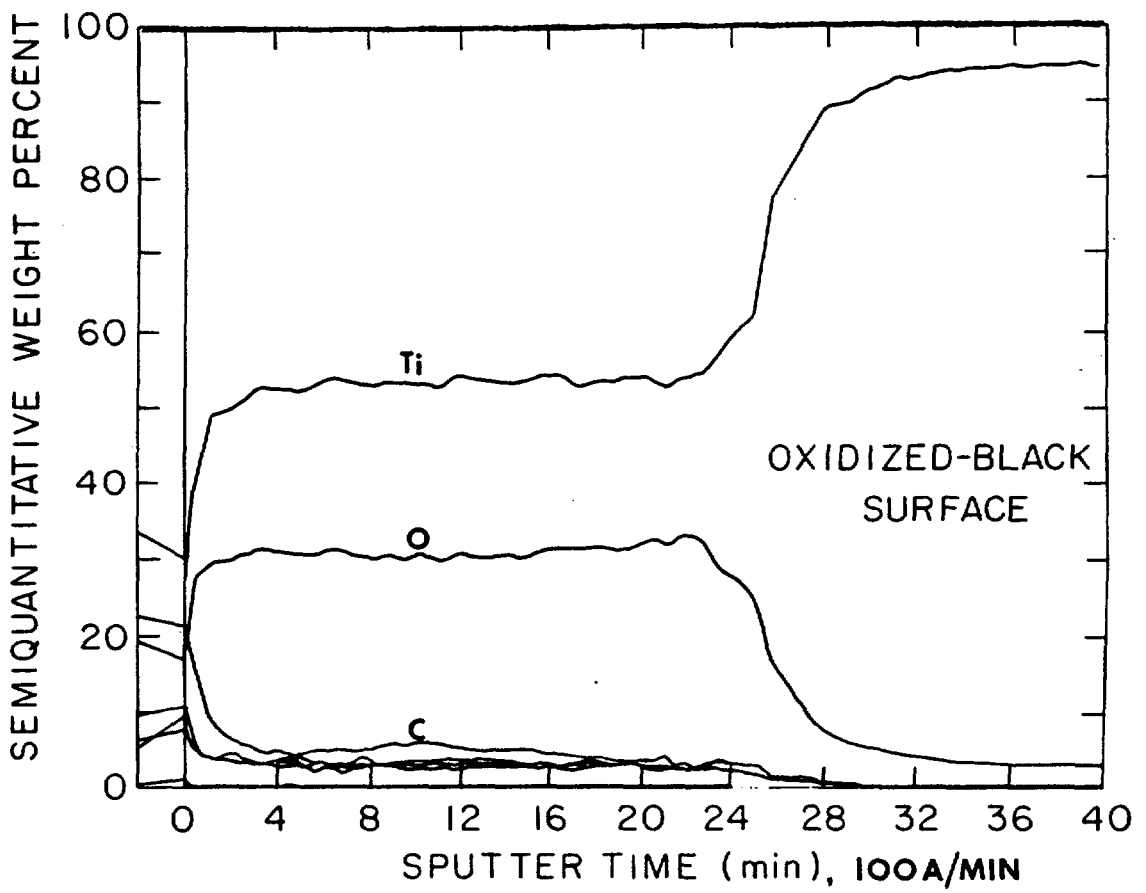

Figure 12. Auger spectrum of the crevice corrosion product and base metal of the sample used for EDAX analysis.

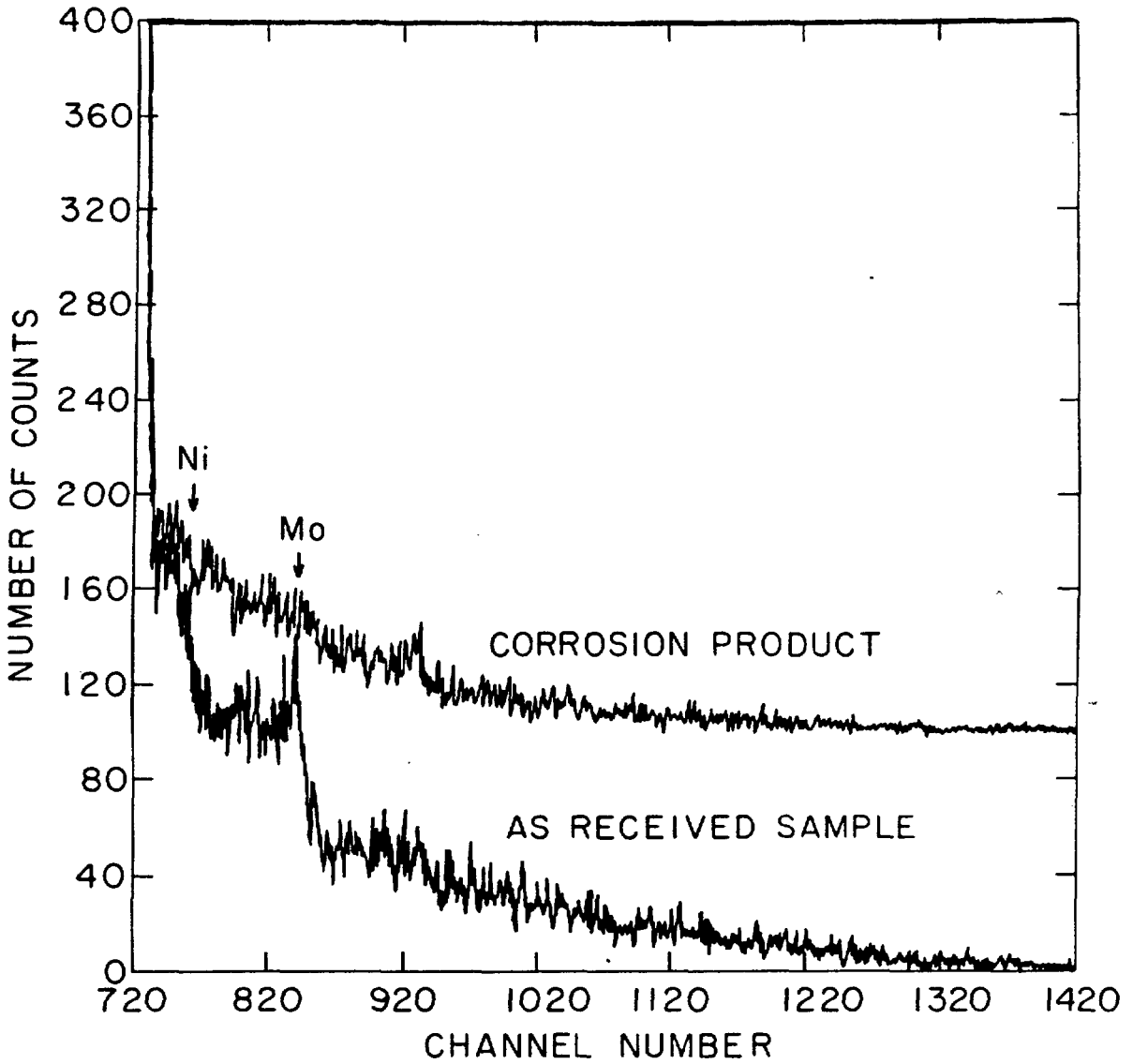

Figure 13. Rutherford backscattering spectrum of the crevice corrosion product of the sample used for EDAX analysis.

5. DISCUSSION

It is evident that the formation of an aeration cell is responsible for crevice corrosion. This follows from the easier initiation, and the higher rates, of crevice corrosion for higher dissolved oxygen concentrations. The concentration of oxygen inside the crevice, compared to the bulk solution, will determine the severity of corrosion for the initial aeration cell. Also, increasing the sample size and decreasing the crevice gap (metal/Teflon samples) gives slower inflow of oxygen into the center of the crevice, leading to more severe corrosion. Temperature effects may also be explained on the basis of the above arguments. Above a certain temperature, the diffusion rates of the dissolved species are faster, and oxygen solubility is decreased. Thus, a concentration cell may not develop easily and this will minimize crevice attack.

The results obtained from the cathodic surface preoxidation test indicate that preoxidation will lead to an increased potential difference between the anodic and cathodic regions, thereby resulting in enhanced crevice attack. The data on solution pH effects imply that it is necessary to attain low pH values within the crevice to cause severe corrosion. When the bulk solution pH is lowered, it is easier to obtain the low pH condition inside the crevice necessary for passivity break-down and subsequent fast dissolution. Since electrical neutrality must be preserved in the crevice, this low pH is accompanied by a high anion (chloride) concentration.

From the above observations, the current work is in qualitative agreement with crevice corrosion mechanism proposed previously. The general sequence of steps in the mechanism may be stated as follows:

1. Oxygen depletion occurs in the crevice
2. Acidity increases and anions accumulate in the crevice
3. Local break down of passive film commences, followed by pit formation and fast dissolution

The potential drop may occur throughout Stage 1 to Stage 3.

In the literature, three different oxides have been reported as possible corrosion products for titanium and its alloys in acidic solution [17,18] or in neutral NaCl solutions [9,18]. These are the stable rutile form of TiO_2 (tetragonal), the metastable anatase form of TiO_2 (tetragonal), and another metastable brookite form of TiO_2 (orthorhombic). The metastable forms have been reported to act as barriers to corrosion and drastically retard the corrosion process [17,18]. On the other hand, rutile is known to be present as a porous layer and possibly orginates for some secondary process such as precipitation [17,18]. Rutile is not an effective barrier to corrosion. Figures 14-16 show the sequence for rutile formation within Grade-12 titanium crevices. Rutile needles are formed on the anatase surface (Figure 14) forming domains (Figure 15) and eventually filling the whole crevice (Figure 16). The thickness of anatase barrier oxide is proportional to the electrode potential increase [17,19,20]. Therefore, we can conclude that the potential will increase in the early stage of crevice corrosion since the formation of the barrier oxide will consume oxygen in the crevice. Such a potential rise has been observed in stainless steel crevice corrosion [21]. After the maximum potential is reached, the barrier oxide ceases to grow, while the porous rutile will form either by the transformation of existing anatase, resulting

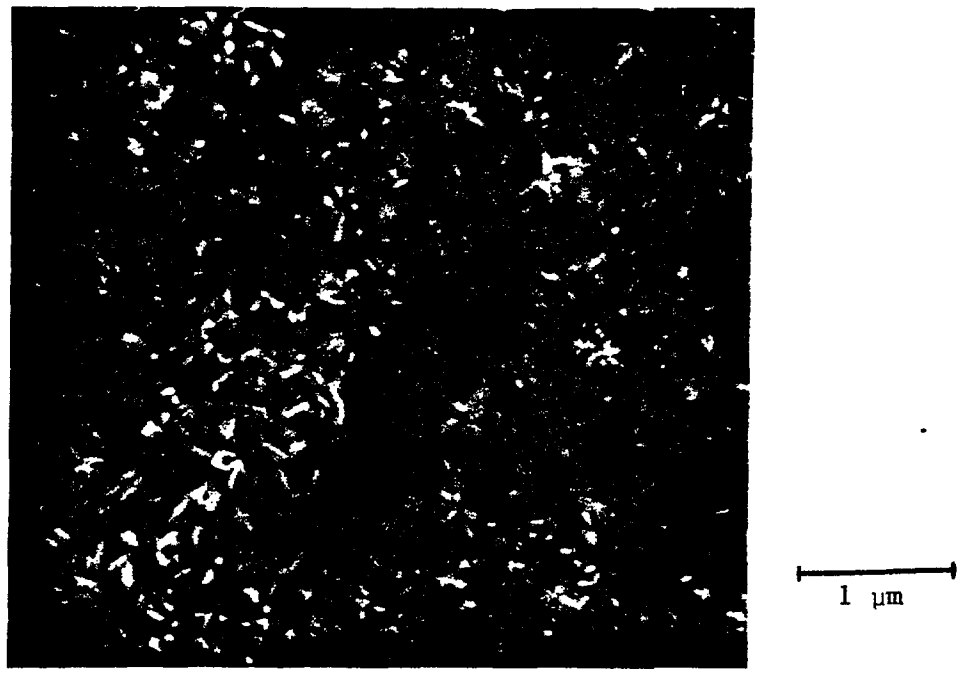

Figure 14. Initial stage of rutile formation of a crevice of ASTM Grade-12 titanium exposed to Brine A at 150°C.

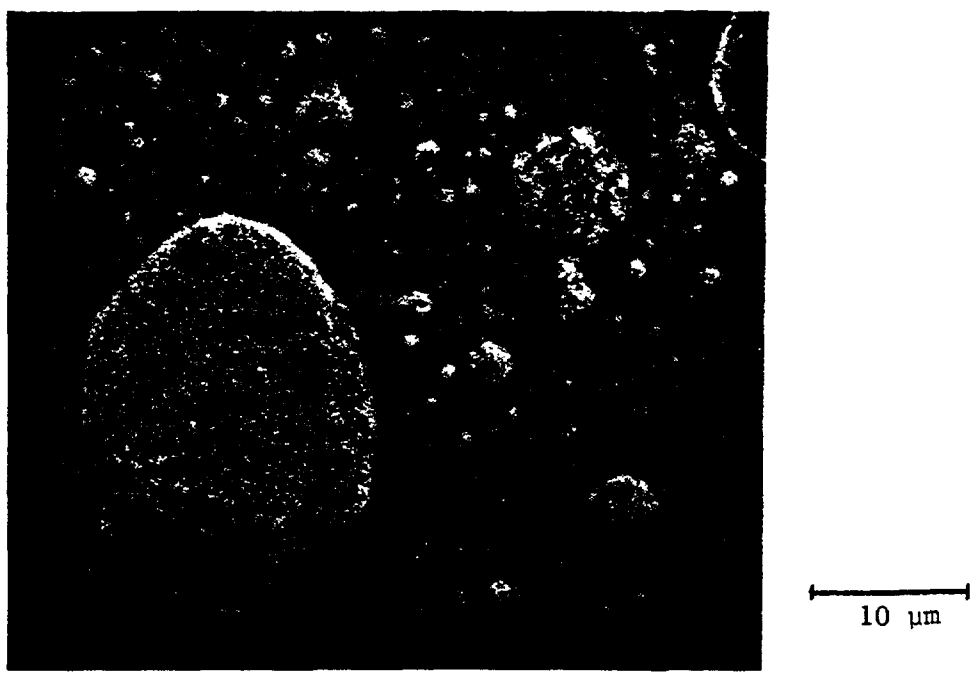

Figure 15. Growing rutile domains in a crevice of ASTM Grade-12 titanium exposed to Brine A at 150°C.

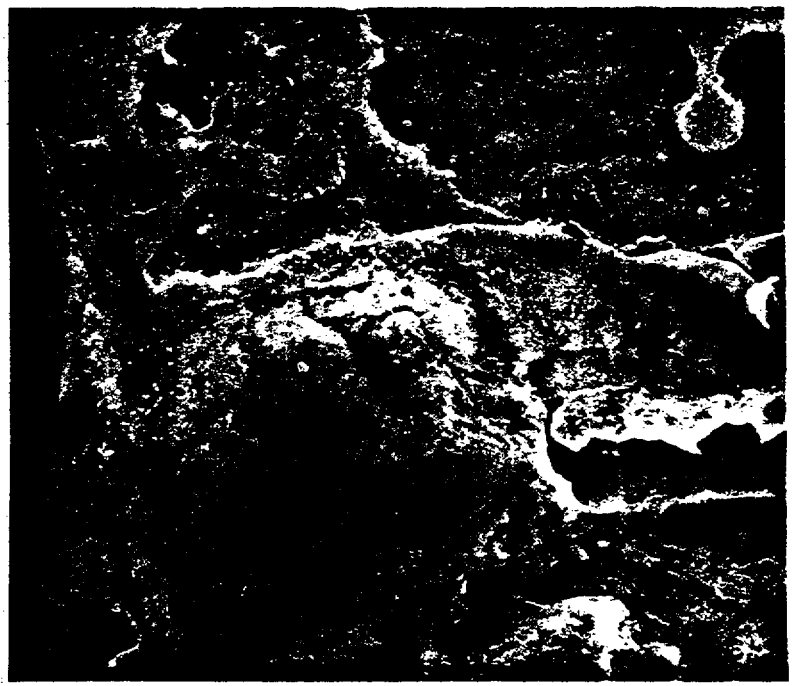

Figure 16. Rutile formed in a crevice of ASTM Grade-12 titanium exposed to Brine A at 150°C filling the whole crevice.

Table 4. Thermodynamic data for the hydrolysis reaction of the probably dissolved ions at room temperature [22].

$Ti^{++} + 2H_2O = TiO_2 + 4H^+ + 2e^-$	$E_o = -0.502 - 0.1182\ pH - 0.0295 \log (Ti^{++})$
$Ti^{+++} + 2H_2O = TiO_2 + 4H^+ + e^-$	$E_o = -0.666 - 0.2364\ pH - 0.0591 \log (Ti^{+++})$
$3Ni^{++} + 4H_2O = Ni_3O_4 + 8H^+ + 2e^-$	$E_o = +1.977 - 0.2364\ pH - 0.0886 \log (Ni^{++})$
$2Ni^{++} + 3H_2O = Ni_2O_3 + 6H^+ + 2e^-$	$E_o = +1.753 - 0.1773\ pH - 0.0591 \log (Ni^{++})$
$Ni^{++} + 2H_2O = NiO_2 + 4H^+ + 2e^-$	$E_o = +1.593 - 0.1182\ pH - 0.0295 \log (Ni^{++})$
$Mo^{+++} + 2H_2O = MoO_2 + 4H^+ + e^-$	$E_o = +0.311 - 0.2364\ pH - 0.0591 \log (Mo^{+++})$

in a potential drop, or by some secondary processes such as precipitation [17,18]. The rutile layer is known to thicken as the electrode potential is decreased [17]. It is important to assess the electrode potential during the initial stage of crevice corrosion in order to identify barrier and non-barrier oxides and to relate their thickness to the electrode potential. This relation will be used later in the calculation of the crevice corrosion potential.

The crevice corrosion products used for the chemical analysis are mainly composed of the rutile form of TiO_2, which is a hydrolysis product of ions dissolved in the crevice solution. In order to evaluate hydrolysis effects, thermodynamic data are given in Table 4 for Ti, Ni and Mo of the probably dissolved ions at room temperature, quoted from reference [22]. A spontaneous hydrolysis reaction is possible for Ti resulting in TiO_2, while any type of nickel oxide will not be formed. For Mo, oxide formation is possible, depending on the local pH variations.

The penetration depth for EDAX analysis is about 4 μm while those for Auger spectroscopy and Rutherford Backscattering are 10 nm and 200 nm respectively. Therefore, Mo is depleted in top 200 nm of the corrosion products near to the solution while the interior of the oxide are enriched with Mo. This may be attributed to the redissolution of Mo by local pH variation although detailed mechanisms are left for future studies.

We now consider how crevice corrosion is activated with respect to the structure and chemistry of oxides formed. Since we have observed quite deep pits, the activation of crevice corrosion is likely to be related to pitting. The pitting can be initiated in different ways for the present crevice

corrosion conditions. For example, as a transient phenomenon from a passive state to an active state. Before the activation of the whole crevice area, the local disappearance of barrier oxide or passive film may have led to the observed pits. In this case, the electrode potential must have been in the active state. Other work [23] shows an active peak for Grade-12 titanium in simulated crevice solutions at 90 - 100°C. An objection to this hypothesis is that the observed pits are too localized with appreciable depths to be considered as a transient phenomenon leading to the overall activation of the whole crevice surfaces. A second hypothesis centers on transpassive pitting. The beta phase is enriched with Mo and the transpassive selective dissolution of Mo has been observed for high Mo-Ti alloys in acidic conditions [24]. Since the region of transpassive behavior for Mo starts at -0.3 V versus SCE in acidic conditions it is quite possible that the pitting potential may have been reached in the beta phase even though the overall pitting potential is in the range of 0.5 to 1.0 volt for simulated crevice solutions [25]. A third possibility involves an anodic, or a transpassive, dissolution of Fe in the beta phase as a galvanic corrosion process. This type of pitting has been reported for shell-and-tube heat exchangers used in 20% CaI_2 brine with small amounts of K^+, Br^-, and I^- [26]. The objection to this hypothesis is that the Fe in Grade-12 titanium is distributed quite uniformly compared to Mo and Ni, as shown in the chemical analysis of the as-received material. From the above discussions on the three hypotheses, it is most likely that crevice corrosion is activated by the initiation in the beta phase. The selective dissolution of the beta phase results in the enrichment of Mo in the crevice corrosion product. The pit initiation may occur locally without being

accompanied by overall thinning of oxide formed in the crevice. In fact, the preservation of overall oxide thickness by uniform dissolution in the crevice has been observed in CP (commercially pure) titanium [27].

We have also studied crevice corrosion of CP titanium [28] in this study. While the CP titanium coupons are nearly destroyed during crevice corrosion, Grade-12 titanium shows very slow crevice corrosion kinetics. It is also possible that crevice corrosion eventually ceases as postulated by other workers [29-32]. Such repassivation has been attributed to Ti^{+4} ion accumulation [29,31], to the formation of polymoybdate species on the metal surface [32], and to salt-layer formation [30]. Discussion of these possibilities will be reported in a subsequent paper [33].

A final point deserves mention in this paper and concerns the use of metal/Teflon crevice samples to obtain a smaller crevice gap compared to those in the metal/metal crevice specimens. The reduced gap has beem shown to give more voluminous corrosion products, but there has long been speculation that the more severe attack comes from fluoride ions released from the Teflon coupon. A recent study on this subject has discarded such a possibility [34]. In this work calcium fluoride was found to have no effect on Ti corrosion performance at high chloride concentrations, which is the case for our study. Therefore, the metal/Teflon crevice sample appears to be an effective method for studying the effects of small crevice gaps on crevice corrosion.

The cation concentration is of less importance in the crevice corrosion process compared to solution pH [9]. Therefore, a few tests in Brine B have shown similar results for Brine A.

6. CONCLUSIONS

Crevice corrosion of ASTM Grade-12 titanium was detected at 150°C in simulated rock salt brine solutions. Lower pH accelerated the reaction rates and deaerated solutions gave less corrosion than aerated ones. Also, increasing specimen size, a decreasing crevice gap, and preoxidation of the cathodic area gave more crevice attack. These results are consistent with those expected from macroscopic concentration cell formation accompanied by oxygen depletion, a potential drop, and acidification inside the crevice. The results of oxide film analysis show that compact anatase crystals are formed initially inside the crevice. As the macroscopic cell develops the beta phase, enriched with Mo and Ni, reaches the transpassive pitting potential causing localized dissolution. During this dissolution, Mo enrichment was observed in the crevice corrosion product. This is caused by the precipitation of dissolved Mo ions. The corrosion product was depleted in Ni since this element is unable to precipitate from the crevice solution. During the dissolution process, rutile crystals are formed in the crevice.

7. REFERENCES

[1] Braithwaite, J. W., N. J. Magnani, and J. W. Munford, "Titanium Alloy Corrosion in Nuclear Waste Environments," Sandia National Laboratories, SAND79-2023C, 1979.

[2] Braithwaite, J. W. and N. J. Magnani, "Nuclear Waste Canister Corrosion Studies Pertinent to Geologic Isolation," Nuclear and Chemical Waste Management, Vol. 1, 1980, p. 37.

[3] Molecke, M. A., D. W. Schaefer, R. S. Glass, and J. A. Ruppen, "Sandia HLW Canister/Overpack Studies Applicable to a Salt Repository," Sandia National Laboratories, SAND81-1585, 1981.

[4] Westerman, R. E., "Investigation of Metallic, Ceramic, and Polymeric Materials for Engineered Barrier Applications in Nuclear Waste Packages," Pacific Northwest Laboratory, PNL-3484, 1980.

[5] Pitman, S. G., "Investigation of Susceptibility of Titanium Grade-2 and Titanium Grade-12 to Environmental Cracking in a Simulated Basalt Repository Environment," Pacific Northwest Laboratory, PNL-39I4, 1981.

[6] Dayal, R., et al., "Nuclear Waste Management Technical Support in the Development of Nuclear Waste Form Criteria for the NRC, Task 1: Waste Package Overview," Brookhaven National Laboratory, NUREG/CR-2333, Vol. 1, BNL-NUREG-51458, 1982.

[7] Ahn, T. M., et al., "Nuclear Waste Management Technical Support in the Development of Nuclear Waste form Criteria for the NRC, Task 4: Test Development Review," Brookhaven National Laboratory, NUREG/CR-2333, Vol. 4, BNL-NUREG-51458, 1982.

[8] Metals Handbook, Vol. 3, Ninth Edition, ASM, Metal Park, OH, 1980, p. 381.

[9] Griess, J. C. Jr., "Crevice Corrosion of Titanium in Aqueous Salt Solutions," Corrosion-NACE, Vol. 24, 1968, p. 96.

[10] Jackson, J. D. and W. K. Boyd, "Crevice Corrosion of Titanium," in Applications Related Phenomena in Titanium Alloys, ASTM STP-43, 1968, p. 218.

[11] Diegle, R. B.., "New Crevice Corrosion Test Cell," Materials Performance, p. 43, 1982.

[12] Posey, F. A. and D. V. Subrahmanyam, "Kinetics of Initiation of Crevice Corrosion of Titanium," ORNL-TM-4099, Oak Ridge National Laboratory, 1973.

[13] Titanium Heat Exchanger for Service in Seawater, Brine, and Other Aqueous Environments," Titanium Information Bulletin from IMI, Birmingham, England, 1979.

[14] Pourbaix, M., Atlas of Electrochemical Equilibria in Aqueous Solutions, 1974, p. 213.

[15] Handbook of Physics and Chemistry, Sixty-Second Edition, CRC Press, 1981-1982, p. B-159-160.

[16] Turner, D. R., "Titanium Etching in Hydrofluoric Acid Solutions," p. 218, vol. 83-2, Extended Abstracts, The Electrochemical Society, Fall Meeting, Washington, D. C., October 9-14, 1983.

[17] Tomashov, N. D., G. P. Cernova, Y. S. Ruscol, and G. A. Ayuyan, "The Passivation of Alloys on Titanium Bases," Electrochemica Acta, Vol. 19, 1974, p. 159

[18] Koizumi, T. and T. Nakayama, "Structure of Oxide Films Formed on Titanium in Boiling Dilute H_2SO_4 and HCl," Corrosion Science, Vol. 8, 1968, p. 195.

[19] McAleer, J. F. and L. M. Peter, "Instability of Anodic Oxide Films on Titanium," J. Electrochemical Society, Vol. 129, No. 6, p. 1252, 1982.

[20] Beck, T. R., "Initial Oxide Growth Rate on Newly Generated Surfaces," J. Electrochemical Society, Vol. 129, No. 11, 1982.

[21] Oldfield, J.W. and W. H. Sutton, "Crevice Corrosion of Stainless Steels, II. Experimental Studies," British Corrosion J. 13, 104, 1978.

[22] Pourbaix, M. Atlas of Electrochemical Equilibria in Aqueous Solutions, NACE, 1974, p. 213, p. 256, p. 307.

[23] Molecke, M. A., "High-Level Waste Packge Materials Quarterly Report," Sandia National Laboratories, July 1983.

[24] Glass, R. S. and Y. K. Hong, "Mechanism of Transpassive Dissolution of Titanium-Molybdenum Alloys," Extended Abstracts, Vol. 83-1, The Electrochemical Society, Spring Meeting, San Francisco, CA, May 8-13, 1983.

[25] Campbell, G., Unpublished Research, Brookhaven National Laboratory, 1983.

[26] Liening, E. L., "Unusual Corrosion Failures of Titanium Chemical Processing Equipment," Materials Performance, p. 37, November 1983.

[27] Shimogori, K., H. Sato and H. Tomari "Crevice Corrosion of Titanium in NaCl Soltions in the Temperature Range 100 to 250°C," Journal of Japan Institute of Metals 42(6), 1978.

[28] Lee, B. S., T. M. Ahn and P. Soo, "Crevice Corrosion of Titanium in a Brine Solution," Extended Abstract in The Symposium of Crevice Corrosion, The Electrochemical Society, Fall Meeting, Detroit, 1982.

[29] Kelly, E. J., "Anodic Dissolution and Passivation of Titanium in Acidic Media III Chloride Solutions," J. Electrochemical Society, Vol. 126, No. 12, p. 2064, 1979.

[30] Beck, T. R., "Pitting of Titanium, 1. Titanium-Foil Experiments," J. Electrochemical Society, Vol. 120, No. 10, p. 1310, 1973.

[31] Thomas, N. T., K. Nobe, "Electrochemical Behavior of Titanium, Effect of Ti(III) and Ti(IV)," J. Electrochemical Society, Vol. 119, No. 11, p. 1450, 1972.

[32] Glass, R. S. "Passivation of Titanium by Molybdate Ion," Extended Abstracts, Vol. 83-2, The Electrochemical Society, Fall Meeting, Washington, DC, October 9-14, 1983.

[33] Jain, H., T. M. Ahn and P. Soo, "Current, Potential and pH Measurements for the Crevice Corrosion of Grade-12 Titanium in a Brine," forthcoming paper.

[34] Thomas, D. E. and H. B. Bomberger, "The Effects of Chlorides and Fluorides on Titanium Alloys in Simulated Scruber Environments," Materials Performance, p. 29, November 1983.

ACKNOWLEDGMENT

This work was performed under the auspices of the Nuclear Regulatory Commission (NRC). The authors acknowledge the program coordination by Drs. K. Kim and M. McNeil of the NRC. Works on Auger Spectroscopy and Rutherford Backscattering were done by D. J. Hunt of Inco and A. L. Hanson of BNL, respectively. Both works will be summarized as technical notes separately.

Brookhaven National Laboratory Report

BNL-NUREG-34791 (1984)

AN ELECTROCHEMICAL STUDY OF CREVICE CORROSION OF GRADE-12 TITANIUM IN A BRINE SOLUTION AT 150°C

H. Jain, T. M. Ahn and P. Soo

Department of Nuclear Energy
Brookhaven National Laboratory
Upton, New York, 11973

Key Description: Titanium, Crevice Corrosion, Electrochemical Study, Occluded Cell

ABSTRACT

The crevice corrosion of Grade-12 titanium has been studied in a simulated rock salt brine of varying acidity and dilution. The stages of corrosion were monitored by continuously recording the crevice potential and current. Initially, the anode potential increased due to the growth of a barrier oxide. After this period, local passivity breakdown occurs accompanied by a potential drop and a current increase. Following breakdown of passivity, the crevice current decreases and the potential increases, suggesting that part of the specimen surface repassivates. However, repassivation seems to be compromised by subsurface cracking during long term testing. The incubation period for crevice corrosion in various solutions was found to be about two-three days. In comparison, the incubation period for Grade-2 titanium is essentially zero and repassivation does not occur. Corrosion rates for this material are much higher. Possible crevice corrosion mechanisms for the two materials are discussed.

FIGURES

1. Schematic diagram of the testing equipment for monitoring crevice corrosion under hydrothermal conditions (a) autoclave and accompanying current/potental measuring assembly. AC: stainless steel autoclave, L: Teflon liner, PLG: pressure gage, RD: rupture disc, GV: gas control valve, TC: chromal-alumel thermocouple encased in titanium sheath, R: Ag/AgCl (saturated KCl) reference electrode, CC and CS: Cathode and anode assembly used in measuring current, PC and PS: cathode and anode assembly used in measuring pH, V: potentiometer, A: Current meter, R: recorder. (b) anode assembly used in current/potential measurements. BA: anode, TP: telfon discs, PP1 and PP2: titanium pressing plates, E: enamel used for electrical insulation. (c) anode assembly used in pH measurements. PA: anode disc, W: wells for collection crevice solution.

2. A Grade-12 titanium anode specimen after the test in dilute (by a factor of 100) Brine A. The white areas represent deposits of TiO_2.

3. A SEM micrograph of a pits formed in the crevice corrosion of Grade-12 titanium (a). When the oxide was removed, the pits formed are more pronounced.

4. A SEM view of the vertical cross section of a corroded area on a Grade-12 titanium anode specimen.

5. An optical micrograph of the surface of a Grade-12 titanium anode specimen showing the corrosion as primarily a pitting phenomenon. Note the alignment of the corrosion.

6. An unusual crater-like feature on the surface of a Grade-12 titanium anode specimen.

7. Time dependence of current and potential for Grade-12 titanium in neutral Brine A. The steady state temperature is ~150°C.

8. Time dependence of current and potential for Grade-12 titanium crevice in diluted (by a factor of two) Brine A. The closed and open circles represent uncoupled potentials of the freely exposed cathode disk and the anode assembly, respectively. The steady state test temperature is ~150°C..

9. Time dependence of current and potentital for Grade-12 titanium in one hundred times diluted Brine A. The closed and open circles represent uncoupled potentials of the freely exposed cathode disk and the anode assembly, respectively. The steady state temperature is ~150°C. The broken line between 90 and 110 hours on the potential curve represents the period during which the potential overshot the recorder scale.

FIGURES (Continued)

TABLES

1. INTRODUCTION

As shown in the previous paper,[1] immersion tests and surface analyses have shown qualitatively that macroscopic concentration cell formation is responsible for Grade-12 titanium crevice corrosion in a simulated rock salt brine at 150°C. Cell formation is accompanied by oxygen depletion, a potential drop, anion accumulation and acidification inside the crevice. This also leads to pit initiation within the crevice. To quantify the crevice corrosion process, in situ electrochemical monitoring is essential. A suitable technique for testing a Grade-12 titanium crevice under hydrothermal conditions was developed.[2] The results of tests on Grade-12 titanium crevices in the simulated rock salt brine are discussed in this paper. The results for Grade-2 titanium crevices are also included for the purpose of comparison.

2. EXPERIMENTAL PROCEDURES

Material and Test Environments

The chemical compositions of Grade-12 and Grade-2 titanium sheet, as supplied by the vendor, are given in Table 1 and the nominal compositions of the simulated rock salt brines were given in the proceeding paper. To lower the pH of this solution, appropriate amounts of hydrochloric acid were added, and to increase its dilution, doubly distilled water was added. All tests were performed in Brine A since it was found that corrosion in the two brines was essentially identical.[1]

Specimen and Cell Design

The specimen and cell designs are based on a simple system for monitoring crevice corrosion viz the freely-exposed cathode and creviced anode are

Table 1. Vendor supplied chemical analysis of Grade-12 and Grade-2 titanium.

	C	Fe	N	Mo	H	O	Ni	Ti
Grade-12 Titanium								
(Current Specimen)[a]	0.009	0.10	0.010	0.27	0.007	0.13	0.84	Balance
(pH Specimen)[b]	0.013	0.13	0.012	0.31	0.008	0.13	0.7	Balance
Grade-2 Titanium								
(Current Specimen)	0.008	0.05	0.004	----	0.005	0.07	----	Balance

[a]For the measurement of crevice corrosion rates.
[b]For the measurement of the pH inside the crevice.

physically separated but connected externally through a current measuring device; a potentiometer monitors the potential with respect to a reference electrode. The current gives an indication of the corrosion rate, whereas the potential can give useful information on crevice conditions. In the present study, the test temperature of 150°C requires the use of an autoclave system. Since Grade-12 titanium is known to be highly corrosion resistant, a very tight crevice is needed to cause attack. This, however, prohibits in situ monitoring of the crevice pH. Consequently, a separate thick crevice specimen with small wells of diameter 0.14 cm was included in the tests to collect a sample of crevice solution, which is used after test completion to measure the pH at room temeprature. The test cell and the configuration of the current and pH specimen assemblies are shown schematically in Figure 1; the details are described elsewhere.(2) All of the cathode and anode specimens are 5-cm diameter discs. The anode specimen is mirror polished to facilitate the formation of a tight crevice when it is sandwiched and pressed between two Teflon discs of the same size. The connecting lead wires made by

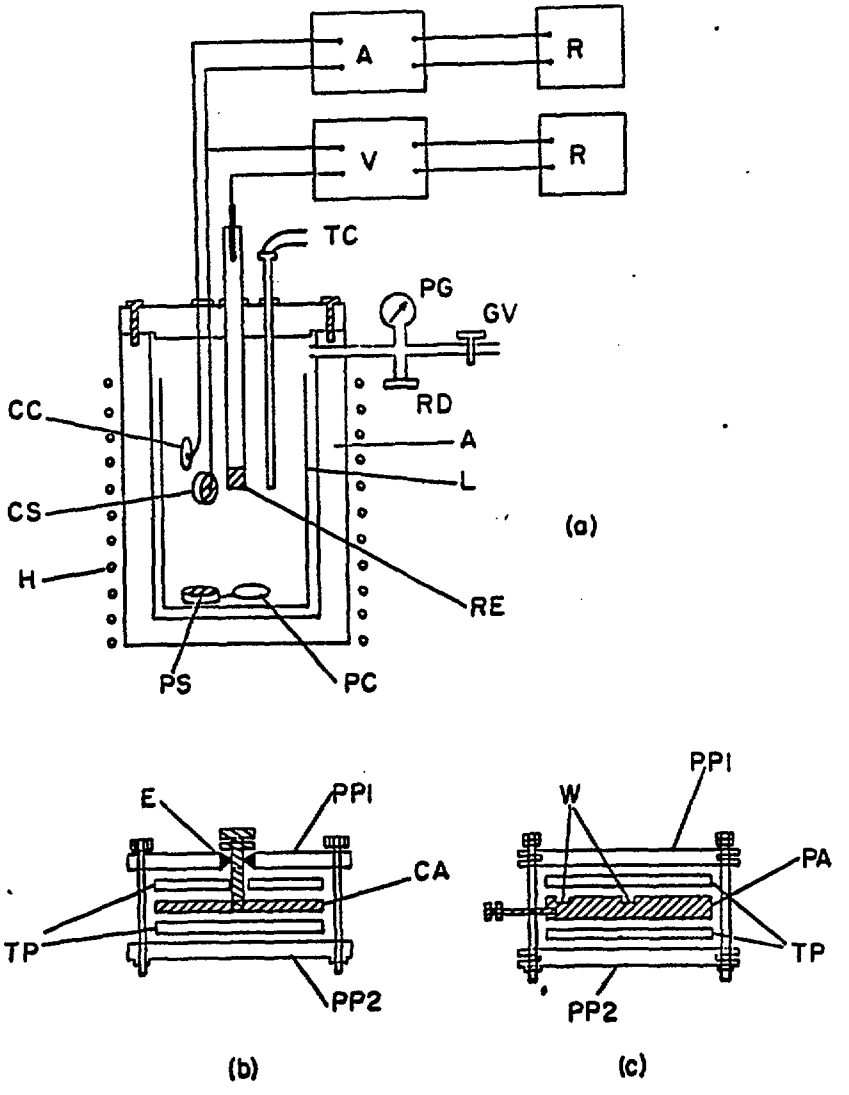

Figure 1. Schematic diagram of the testing equipment for monitoring crevice corrosion under hydrothermal conditions (a) autoclave and accompanying current/potental measuring assembly. AC: stainless steel autoclave, L: Teflon liner, PLG: pressure gage, RD: rupture disc, GV: gas control valve, TC: chromal-alumel thermocouple encased in titanium sheath, R: Ag/AgCl (saturated KCl) reference electrode, CC and CS: Cathode and anode assembly used in measuring current, PC and PS: cathode and anode assembly used in measuring pH, V: potentiometer, A: Current meter, R: recorder. (b) anode assembly used in current/potential measurements. BA: anode, TP: telfon discs, PP1 and PP2: titanium pressing plates, E: enamel used for electrical insulation. (c) anode assembly used in pH measurements. PA: anode disc, W: wells for collection crevice solution.

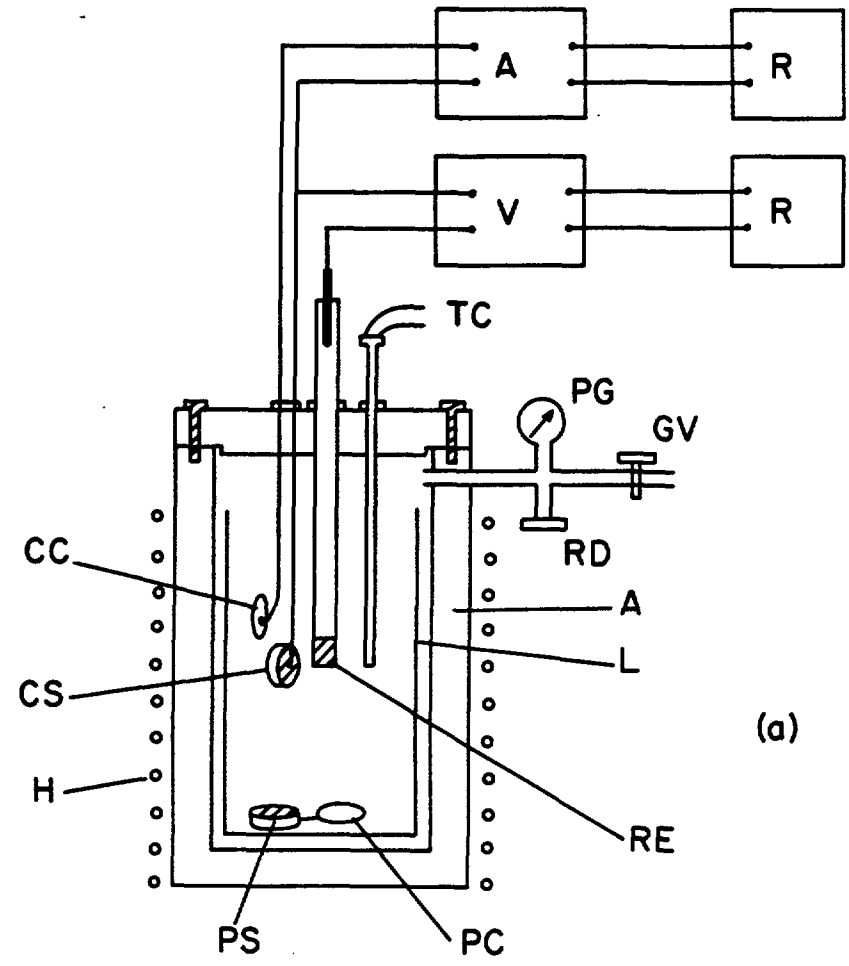

(a)

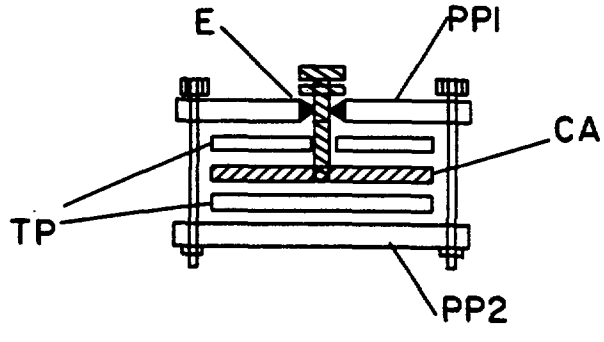

(b)

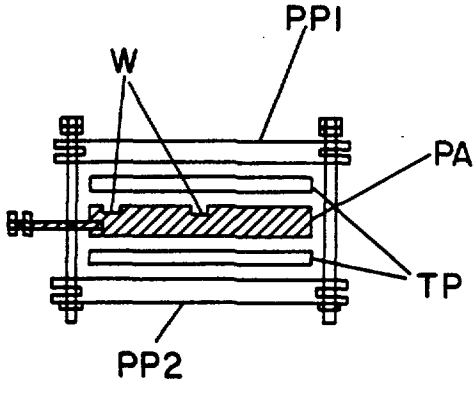

(c)

drawing the alloy sheet, are insulated from the test solution. In this configuation both sides of an anode disc form crevices and, therefore, neglecting the edge area the total anode and cathode areas are equal. The corrosiveness of the brine solution required the use of a Teflon liner and the chromel-alumel thermocouple was encased in a titanium tube.

The potentials are measured with respect to a Ag/AgCl reference electrode (encased in a teflon tube containing saturated KCl) which remains in contact with the test solution through a porous zirconia plug at its lower end. Because of the need for a very tight crevice, the reference electrode could not be placed inside the crevice. The measured potential may include a junction potential when the crevice chemistry has changed from the bulk composition. However, it is expected to be small due to the high ionic concentration of the bulk solution. Recent work by Taylor[3] confirms this.

Test Procedure

Both the current and the pH-anode specimens were assembled as shown in Figures 1b and 1c, respectively, after submerging in the test solution. This eliminated any uncertainty associated with the initial ingress of solution into the crevice. Before sealing the autoclave, the brine solution was oxygenated by bubbling oxygen through it for a minimum time of one hour. The electrical connections were then made as shown in Figure 1a, and the autoclave was heated to ~150°C. The equilibrium pressure of brine at this temperature was approximately 60 psig.

During the test period, which typically lasted for two weeks, the current between the cathode and anode specimens and the potential of the coupled assembly were continuously recorded. Occasionally, the cathode and anode

specimens were decoupled for a few minutes during which the potential of the two electrodes reached stationary values; these were recorded. The usual connections were then restored, and the system returned to coupled condition within a few minutes.

At the end of a test the autoclave was quickly cooled by submerging its lower part in ice cold water. As soon as the temperature fell below the atmospheric boiling point of brine, a gas sample was collected to determine if any hydrogen was generated during corrosion. Then the autoclave was opened and the pH-anode assembly was quenched in a dewar of liquid nitrogen to minimize further alteration of crevice solution characteristics. Subsequently, this assembly was dismantled and the crevice solution in the wells was warmed up to room temperature. Its pH was measured with a microcombination probe (Model MI-410, Microelectrodes Inc.). Due to the condensation of atmospheric moisture on the specimen surface, the observed pH is expected to be an upper limit for the true value.

Finally, the cathode and anode specimens were ultrasonically cleaned in distilled water, dried in air and weighed. The anode specimens were also examined under optical and scanning electron microscopes to study morphological features of corrosion. The depth of crevice attack was determined by sectioning a specimen and examining it with a microscope. In the case of Grade-2 titanium, corrosion was much more severe, which permitted the examination of the corrosion product by X-ray diffraction powder methods.

3. RESULTS

Corrosion Product Morphology

A visual examination of Grade-12 titanium anode specimens showed that crevice corrosion occurs in a non-uniform manner. As shown in Figure 2, a white corrosion product, identified later as the rutile form of TiO_2, was usually present in larger amounts near the edge of the specimen where pressure from the screws is higher. In pH specimens the area near the wells, which has a relatively large volume of the crevice solution, showed the least amount of corrosion. Therefore, it is clear that the crevice gap is very important in determining the extent of corrosion.

A microscopic examination of the corroded surface showed that the corrosion starts in isolated areas presumably with the formation of a pit such as that shown in Figure 3. As corrosion proceeds the pits are filled by the growth of insoluble rutile (TiO_2). Since the oxidation of titanium to rutile is accompanied by a 5.3% increase in volume, a pit is soon covered with TiO_2, forming a mass extending into the crevice. A vertical cross-section of a typical corroded area is shown in Figure 4 where the pit is very shallow and the corrosion product can be seen both above (area a) and below (area b). Note that the volume expansion during corrosion produces stresses high enough to generate a crack (below area c) which can act as a site for crevice corrosion. The corrosion product and the underlying pit were found to be aligned along scratches in the adjacent Teflon disc (Figure 5). This figure also shows the corrosion is primarily a pitting phenomenon under the crevice conditions.

Figure 2. A Grade-12 titanium anode specimen after the test in dilute (by a factor of 100) Brine A. The white areas represent deposits of TiO_2.

(a)

(b)

Figure 3. A SEM micrograph of a pits formed in the crevice corrosion of Grade-12 titanium (a). When the oxide was removed, the pits formed are more pronounced (b).

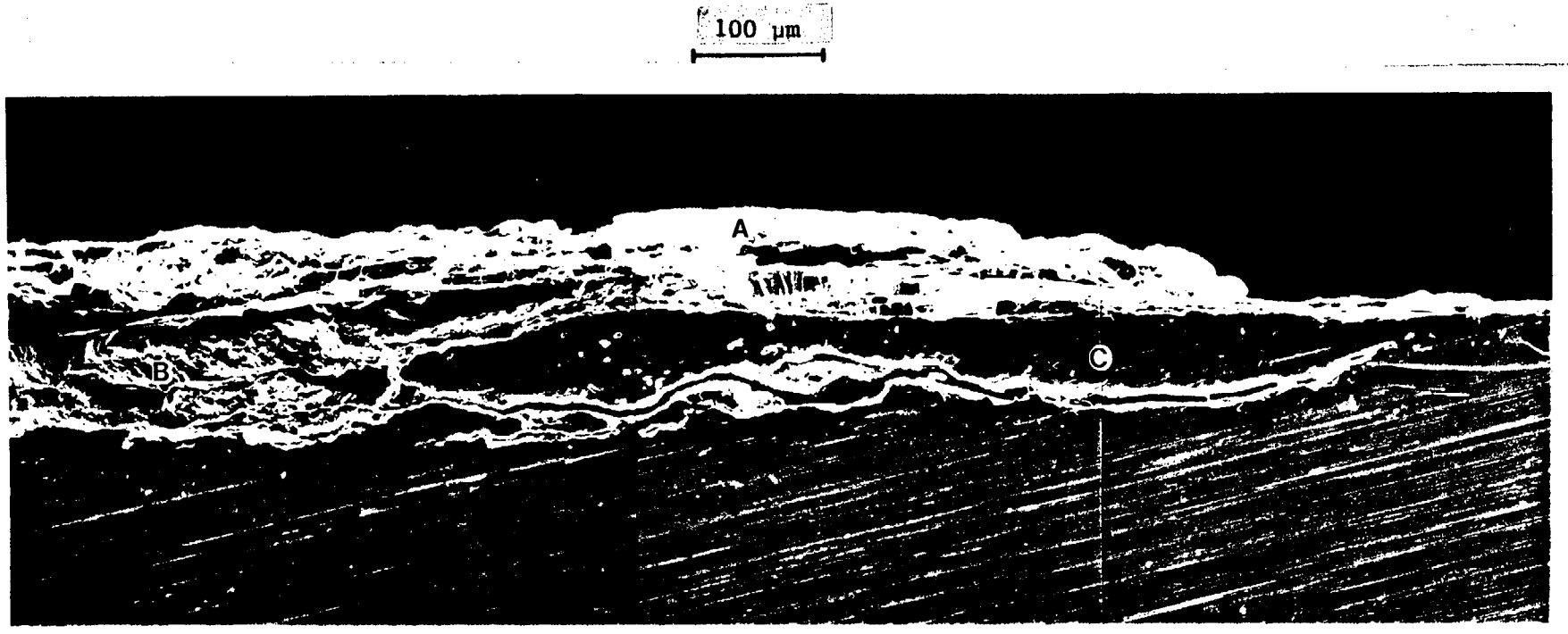

Figure 4. A SEM view of the vertical cross section of a corroded area on a Grade-12 titanium anode specimen.

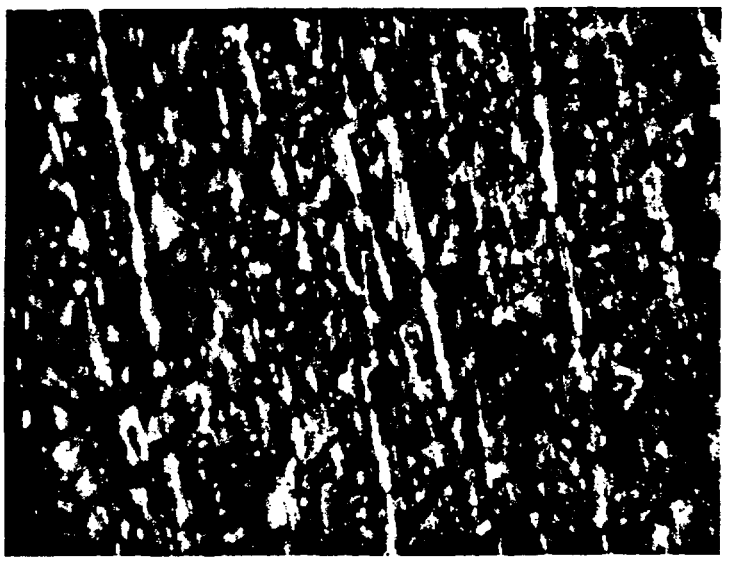

Figure 5. An optical micrograph of the surface of a Grade-12 titanium anode specimen showing the corrosion as primarily a pitting phenomenon. Note the alignment of the corrosion.

Figure 6 shows an unusual crater-like feature on the surface of a Grade-12 titanium anode specimen. It appears that an oxide dome was formed due to the initial corrosion and at a later time corrosion restarted at the bottom of the pit. As in the case of Grade-12 titanium, the crevice corrosion of Grade-2 titanium was relatively severe near the edge of the specimen. However, in this case, it was much more severe so that the edge area had broken into brittle fragments. In general, the cathode specimens of both metals developed a strongly adhering uniform oxide film, but in the case of Grade-2 titanium there was an unexpected observation of the loss of metal from an area on the edge of the specimen.

Weight and pH Measurements

The weights of both the Grade-12 titanium current and pH anode specimens increased as a result of corrosion. Generally, the weight increase for the

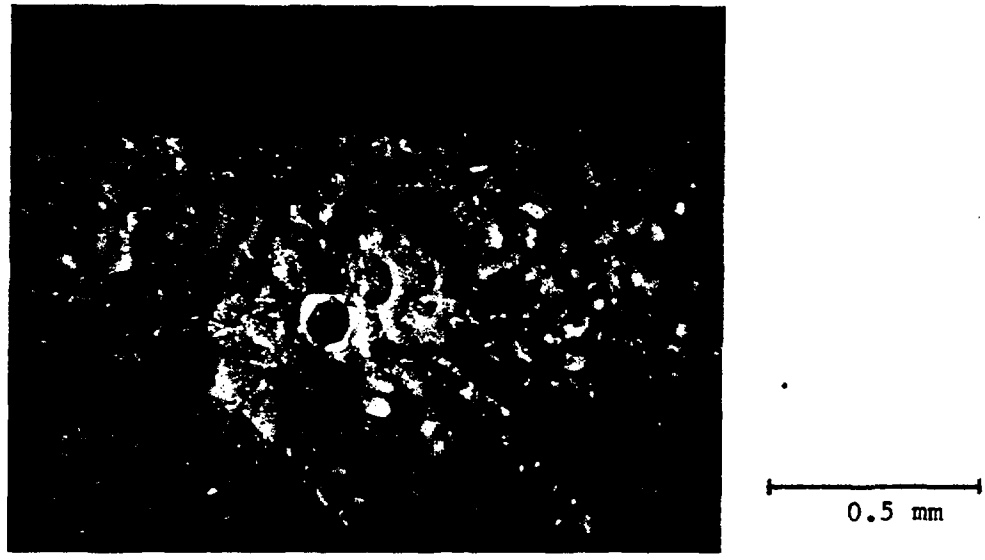

Figure 6. An unusual crater-like feature on the surface of a Grade-12 titanium anode specimen.

current-anode was about one and a half times less than that for the pH-anode specimen (Table 2). This difference may be due to any existing resistance of the connecting path between cathode and anode in the case of current measuring crevice configuration. However, no significant potential drop is observed across the ammeter and path between two electrodes. Alternatively, if the cathodic reaction is significant at the freely exposed edge of anode, it will be greater in the case of much thicker pH-anode specimen. The weight increase for cathode specimens, which showed a uniform tarnish after the test, was approximately two orders of magnitude smaller than that for the anode specimens.

As mentioned previously, the anode specimen used in the Grade-2 titanium crevice was corroded to such an extent that part of it fractured and became detached from the sample. After simple scraping, some of the corrosion product was still attached but the specimen showed a weight loss of 6.8%.

Table 2. pH of the crevice solution and weight gain of the crevice anode after two-week tests in three brines.

Bulk Solution	Starting Bulk Solution pH	Crevice Solution pH	Weight Gain of pH Specimen (g/cm^2)
Neutral Brine A	7.0	3.2	7.0×10^{-4}
Acidic Brine A	4.2	3.8	9.5×10^{-4}
Ten Times Diluted Brine A	8.4	2.8	12.3×10^{-4}
One Hundred Times Diluted Brine A	---	---	10.9×10^{-4}

The results of the room temperature pH measurements on the starting bulk solution as well as the crevice solution after test are given in Table 2. The pH values at the test temperature are expected to be lower.[4] Since the extent of crevice corrosion was usually smaller around the pH wells, the lowering of pH due to corrosion would be less in this area and, therefore, these values represent an upper limit for the actual pH in the more corroded areas. In the case of ten times diluted Brine A, the pH of condensed moisture in the uniformly corroded area was as low as 1.8. The condensed moisture outside the crevice had a pH of 5.9.

Potential and Current Measurements

The variation with time of the potential of the cathode/anode coupled assembly, and the current from the cathode to the anode specimen for Grade-12 titanium crevice in neutral Brine A is shown in Figure 7. The behavior of similar crevices in the ten times and the one-hundred times diluted Brine A are shown in Figures 8 and 9. It also shows the uncoupled potentials of the cathode and anode specimens, which were recorded after decoupling the two for

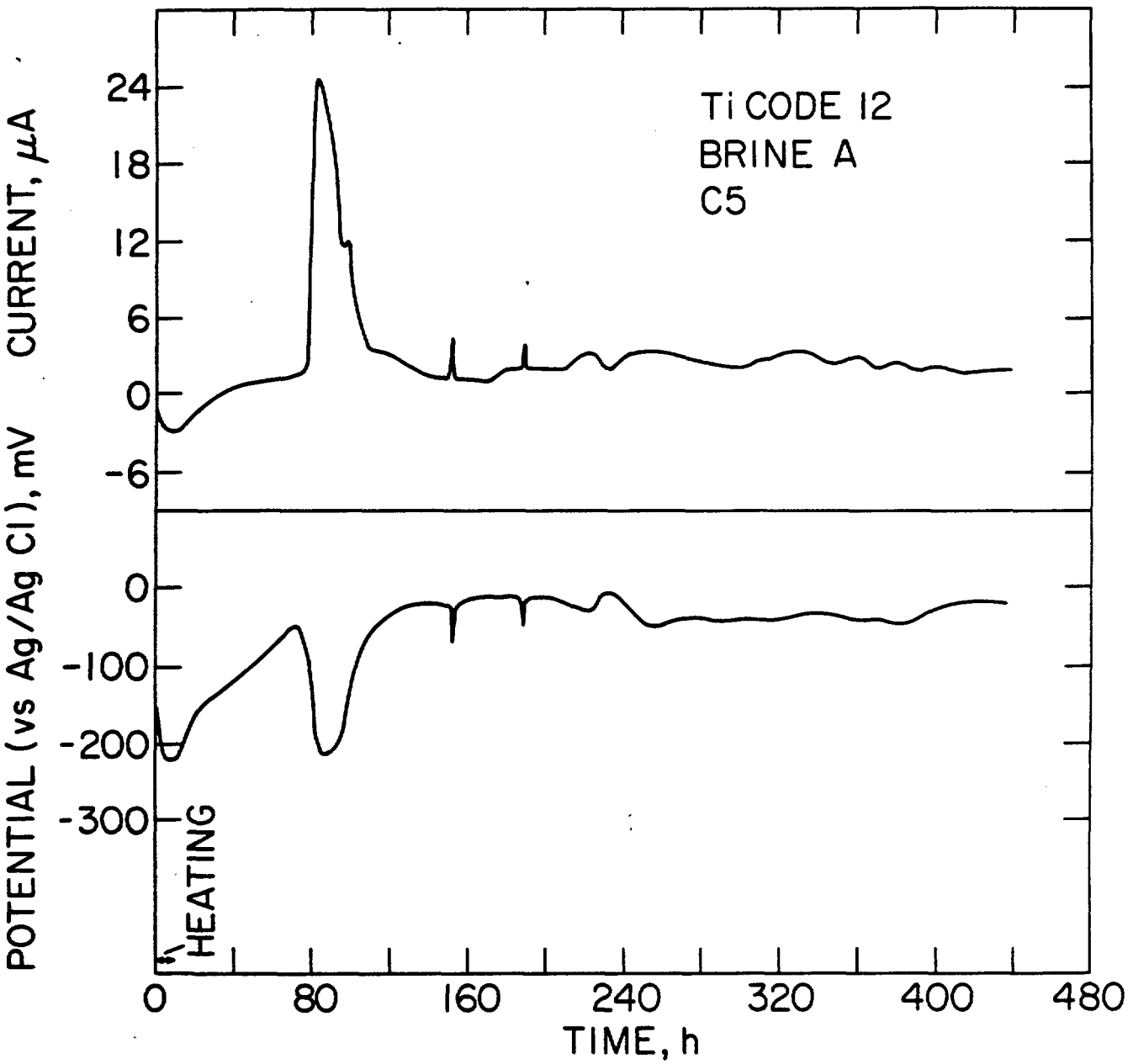

Figure 7. Time dependence of current and potential for Grade-12 titanium in neutral Brine A. The steady state temperature is ~150°C.

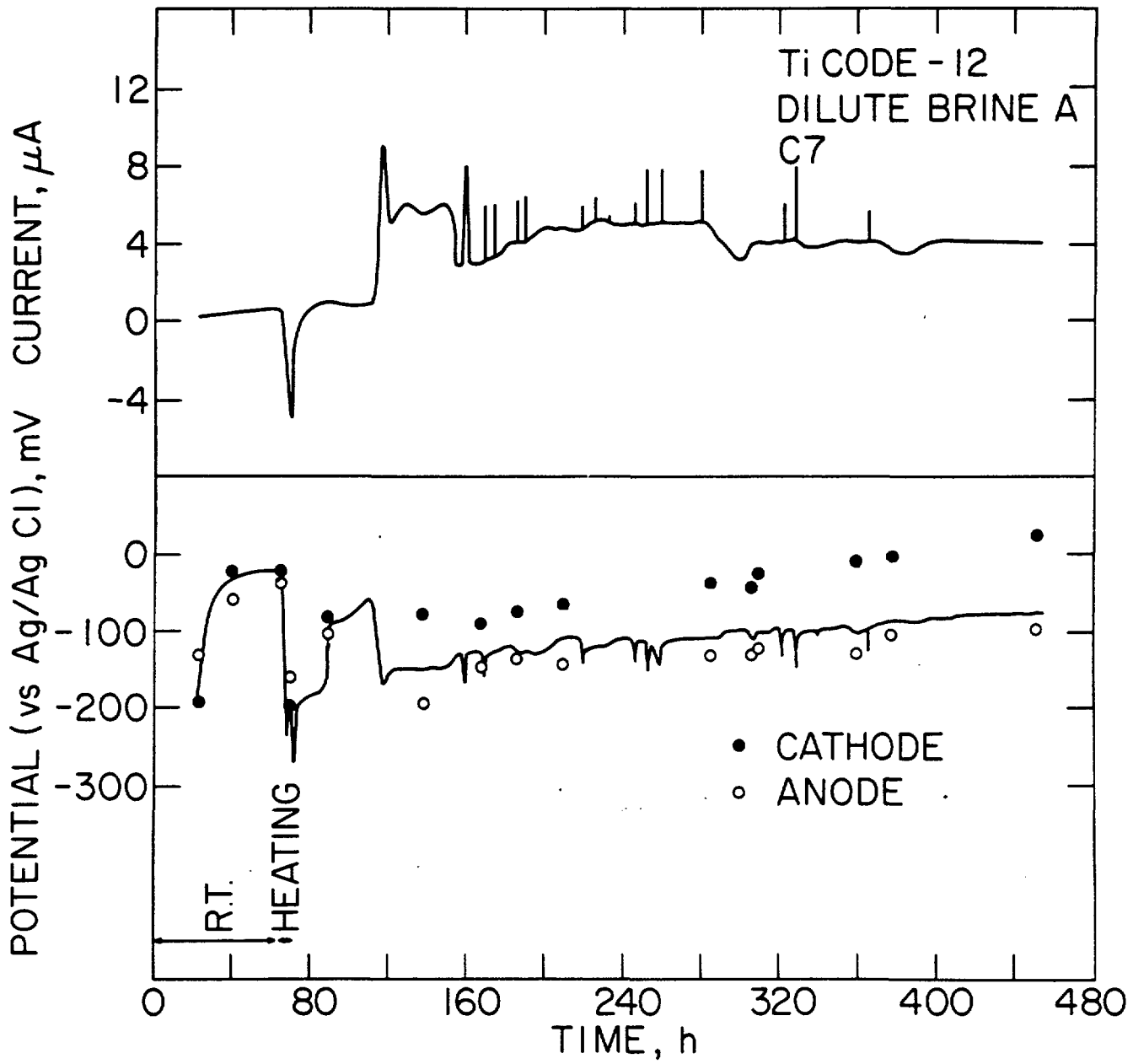

Figure 8. Time dependence of current and potential for Grade-12 titanium crevice in diluted (by a factor of two) Brine A. The closed and open circles represent uncoupled potentials of the freely exposed cathode disk and the anode assembly, respectively. The steady state test temperature is ~150°C..

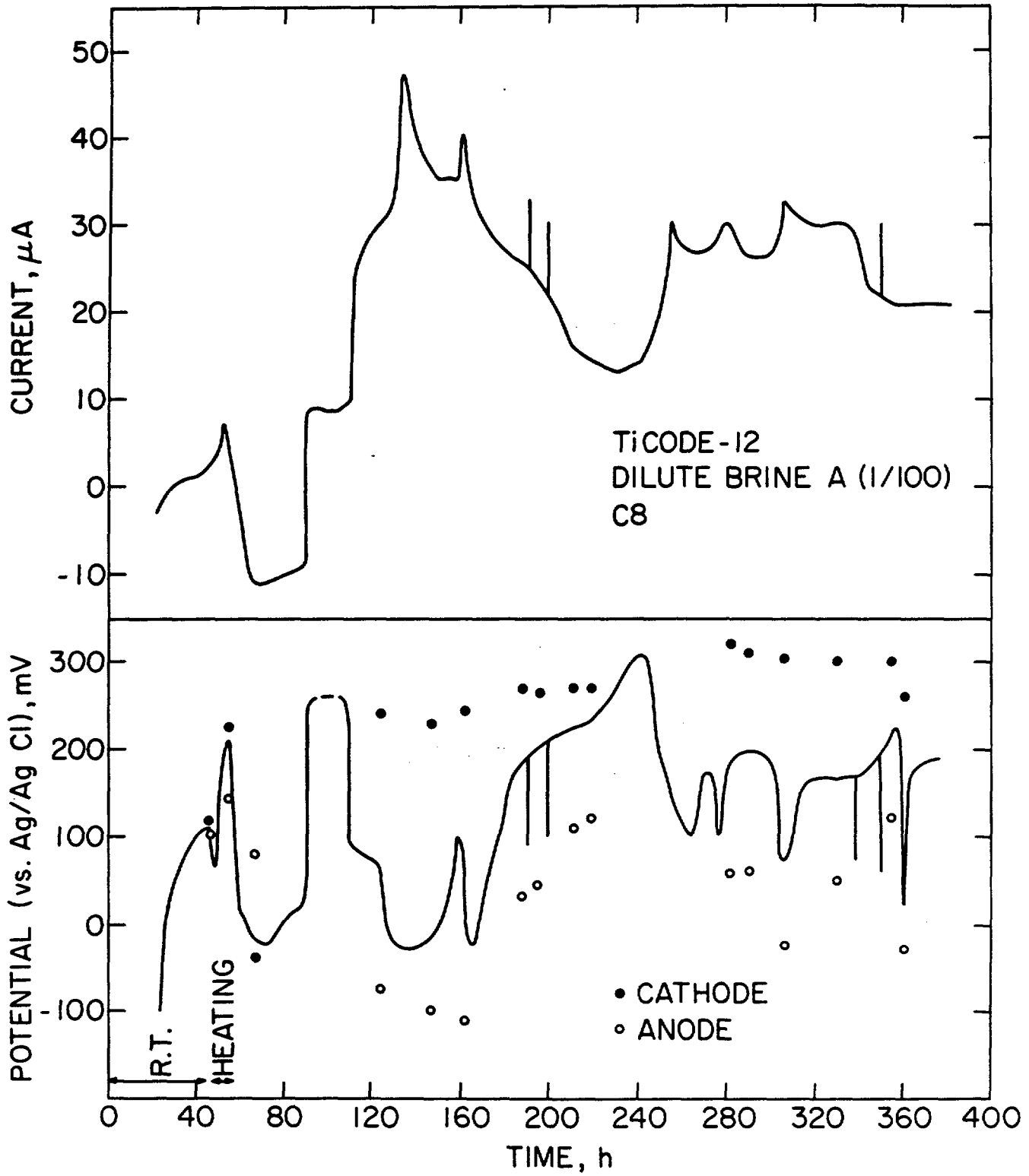

Figure 9. Time dependence of current and potentital for Grade-12 titanium in one hundred times diluted Brine A. The closed and open circles represent uncoupled potentials of the freely exposed cathode disk and the anode assembly, respectively. The steady state temperature is ~150°C. The broken line between 90 and 110 hours on the potential curve represents the period during which the potential overshot the recorder scale.

a few minutes. Note that the cathode potential shows a much smaller change, whereas the anode potential nearly follows the pattern of the coupled potential. Similar curves were obtained for Grade-12 titanium crevices in acidic (pH = 4.2) Brine A as shown in Figure 10. Initially, such current and potential behavior appears to be complex, but a closer examination suggests the following common features:

(a) Initially, when the autoclave is at room temperature, the coupled potential increases at a rate which decreases with time, whereas the current remains essentially zero.

(b) As the autoclave is heated, a negative current accompanied by a sharp decrease in crevice potential is recorded. The difference between the individual potentials of cathode and anode specimens becomes larger.

(c) After the autoclave has reached the test temperature, the potential rises and the current becomes significantly lower. Occasionally, the negative current proceeds the low positive current (Figure 9).

(d) Later, the current shows an abrupt increase which is accompanied by a decrease in crevice potential.

(e) In the following period which covers most of the test time, the current and potential do not show any reproducible behavior. However, an increase in current is always accompanied by a decrease in coupled potential. For the case of neutral Brine A (Figure 7). the current slowly decreased to a very small value. For ten-times diluted Brine A and acidic Brine A, this attentuation of current was intermediate between the patterns shown in Figures 8 and 10.

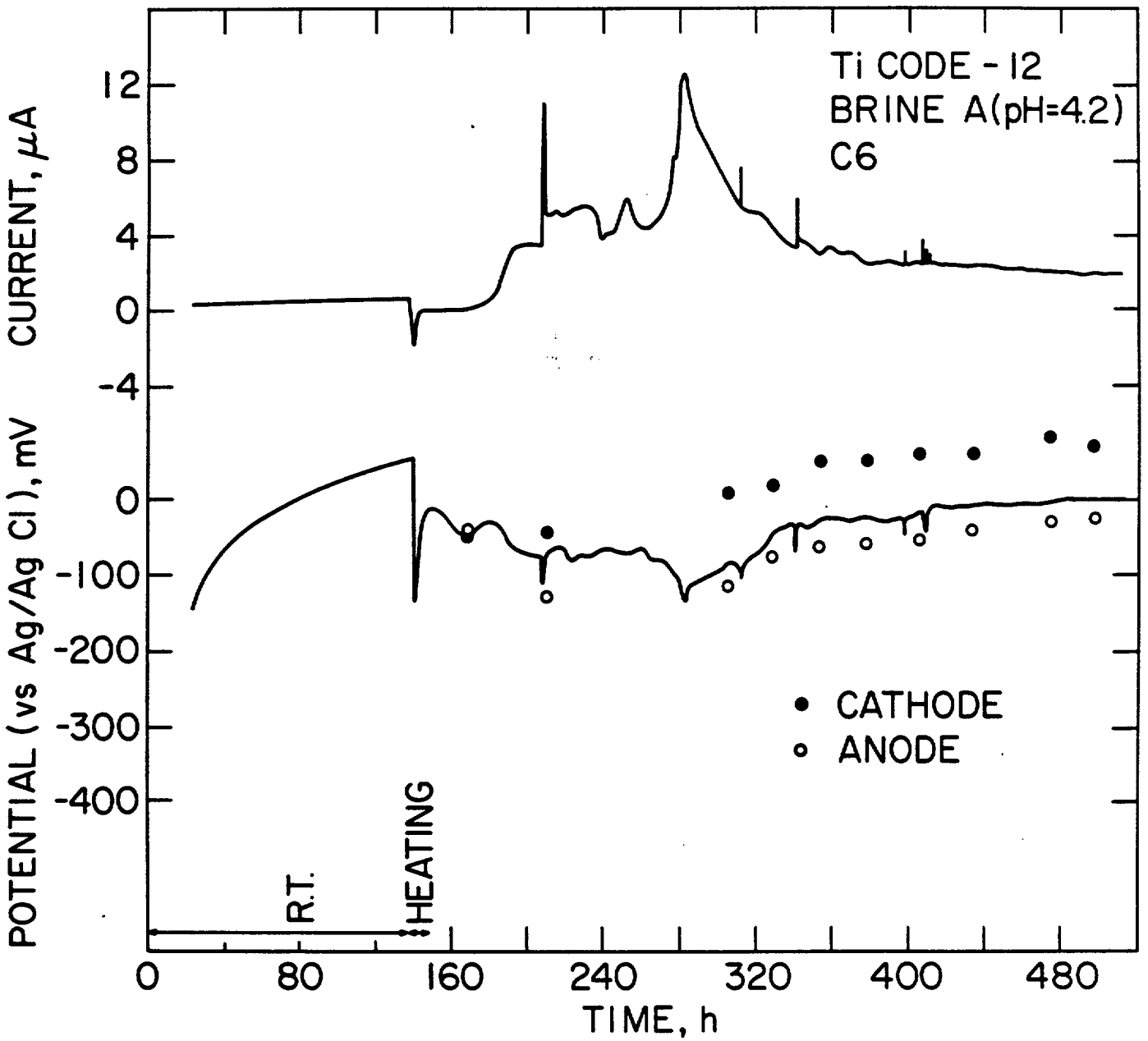

Figure 10. Time dependence of corrosion current and potentital of Grade-12 titanium in acidified Brine A at 150°C. Circles represent the decoupled potentials.

The time dependence of current and potential for Grade-2 titanium crevice in neutral Brine A is shown in Figure 11. In this case the decoupled potentials were not recorded. The figures show several important differences compared to Grade-12 titanium crevices. Firstly, the crevice current is approximately three orders of magnitude higher. Secondly, the above described steps (b) and (c) were not detected; instead step (d) is observed during the heating period. Thirdly, after about 110 hours, the crevice current decreases but it is not accompanied by any potential increase. Finally, after approximately 125 hours the current not only approaches zero, but changes polarity.

4. DISCUSSION

Metallographic examination (Figure 2) confirms ear ier o servations[1,5] that Grade-12 titanium is susceptible to crevice corrosion in Brine A at 150°C. As shown by the less severe corrosion near the pH wells and the more severe corrosion near the edges of the specimens where pressure from the screws was higher, one of the most important conditions for observing crevice attack is the presence of an extremely narrow crevice gap.

The sequence of crevice corrosion for Grade-12 titanium as shown by the time dependent behavior of crevice potential and current (Figures 7 to 10) is in general agreement with the crevice corrosion model decribed in the preceding paper. However, some additional details of the corrosion mechanism can be obtained from the present data.

Initially, at room temeprature, the coupled potential gradually increases with the growth of a barrier oxide.[1] If the cathode and anode specimens have different starting surface conditions, their decoupled potentials would

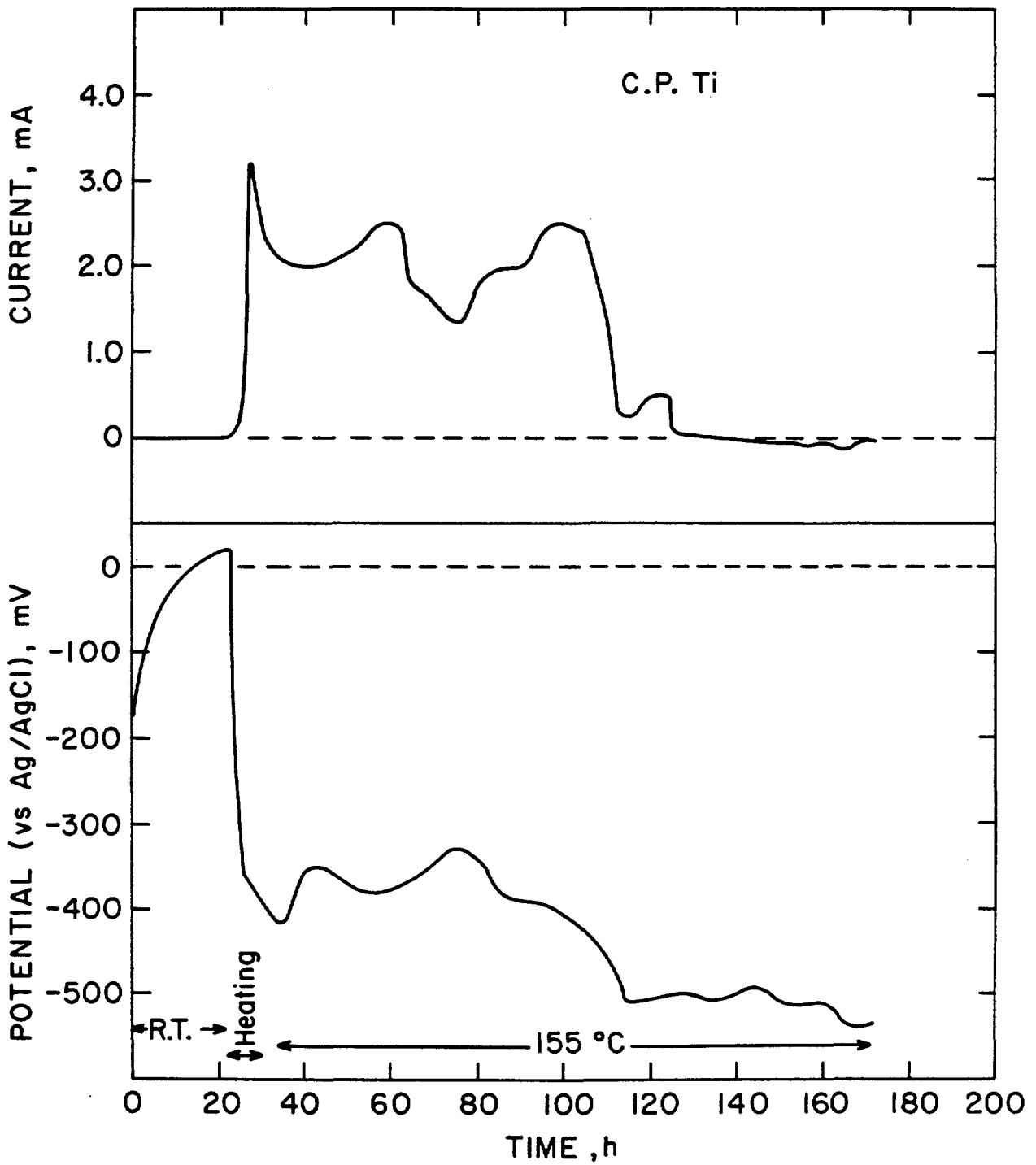

Figure 11. Time dependence of current and potential for Grade-2 titanium in Brine A at steady state temperature 150°C.

be different. (The rate of oxidation at the cathode and anode specimens is about the same so that the crevice current remains negligible.)

During the transient period of autoclave heating, the crevice potential decreases because of adjustment to new equilibrium conditions. At high temperatures the rate of oxide growth is faster and, therefore, the potential starts increasing at a higher rate than at room temperature. However, due to limited availability of oxygen within the crevice, oxide film growth is faster on the cathode than on the anode specimen. Accordingly, the difference between the decoupled cathode and anode specimen potentials becomes larger with time.

After the transient period, the cathode potential occasionally shows a large drop which causes a reversal of the current direction. The reason for this observation is not clear. This phenomenon, when it exists, later disappears and the system reverts back to a normal condition, i.e., the crevice potential rises and the current approaches a small positive value. Under these conditions the crevice chemistry becomes increasingly corrosive, although when a crevice was opened at this stage, only a uniform oxide film was observed. Thus, the crevice corrosion process is still in the incubation phase. With time the crevice solution becomes sufficiently aggressive such that the protective oxide film becomes unstable and fresh metal is exposed. This can be considered to be the end of the incubation period for crevice corrosion. At this point a higher current starts flowing, the potential decreases sharply, and the propagation stage commences. If the oxide film is dissolved only in a small area, then the local metal potential in that area may be even more negative than the observed decoupled anode potential. The

cathode and anode are now permanently separated, the latter being at a much lower potential.

Extensive tests at TIMET[6] have shown that temperature is a very important parameter for the occurrence of crevice corrosion of titanium, and no corrosion in chloride-containing environments is observed at room temperature. Therefore, to estimate the incubation period in the present experiments, we may assume that it starts when the autoclave reaches the test temperature, and ends with the sudden increase in current. With this definition the incubation periods for the neutral, acidic, and ten- and one-hundred-times diluted Brine A are determined to be 68, 45, 44 and 55 hours, respectively. Within the uncertainty in the experimental variables these values are similar. We may, therefore, conclude that as far as the incubation period is concerned all the solutions are equally corrosive. This conclusion implies that the oxygen depletion stage is a rate limiting step for determining the incubation time. The kinetics of anion and proton accumulation are too fast to be observed in the incubation time.

After the breakdown of passivity, the current shows random fluctuations. It is reasonable to believe that the sudden spikes in current which are always accompanied by a sharp decrease in crevice potential correspond to the breakdown of the passive film in discrete areas within the crevice. In the propagation stage large currents flow because the decoupled anode potential has decreased; the cathode potential shows only small changes which are probably due to temperature fluctuations. Isolated occurrence of corrosion within the crevice is also clear from the visual examination of the specimens (Figure 2).

The formation of a pit inside the crevice, as shown in Figure 3, is the first visual sign of crevice corrosion of Grade-12 titanium. At a later stage the anode surface under a microscope shows numerous but generally isolated islands of corrosion product, suggesting that pitting is the precursor of crevice corrosion. The corrosion product which has been identified as the rutile form of TiO_2 soon fills a pit, thereby producing even more severe crevice conditions locally. As shown in the cross section through a typical pit, in Figure 4, the pit is quite shallow. This probably occurs because the TiO_2 formed has a larger volume than the titanium from which it formed and this would reduce the supply of oxygen to the bottom of the pit. The pit would, therefore, tend to grow laterally.

Oldfield and Sutton[7] have previously proposed for the crevice corrosion of Type 316 stainless steel in chloride solutions that the sharp decrease in potential at the end of the incubation period is due to the micropitting of the specimen surface. However, these micropits soon coalesce as the potental approaches a steady state. In the present study, however, we find isolated pits are present several days after the lowering of the crevice potential, and they remain localized. This observation implies that the potential drop is associated with both solution chemistry changes and pit initiation phenomena.

A common feature of all the tests on Grade-12 titanium crevices is that after an initial current increase at breakdown of passivity the current decreases slowly. This phenomenon is most evident in Figure 7 where the current becomes negligible within twenty hours of breakdown; the same is observed for the case of acidic Brine A (Figure 10). For the ten-times diluted Brine A

(Figure 8), the final magnitude of current is relatively large. And for the hundred-times diluted Brine A (Figure 9), there is a second major increase. The large current for hundred-times diluted solution seems to be due to decreased oxygen solubility somehow related to anions concentrations providing larger area for pit initiation. One possible reason for the decrease in current is that the conduction volume within the crevice is reduced by the conversion of titanium to rutile. However, the decrease in current is much greater than can be explained by this mechanism alone. The second increase in current in Figure 9 is also inconsistent with this explanation. Moreover, the accompanying rise in anode potential implies that this decrease is due to some electrochemical change occurring within the crevice, such as repassivation, at least in part of the crevice. Kelly[8] has shown that a titanium surface actively corroding in an acidic medium to form Ti^{+3} can be repassivated if the local concentration of Ti^{+4} ions exceeds a critical value which is determined by the properties of the crevice solution. Such details are not known for the present crevice solutions, but the results show that this self-healing is more easily achieved in neutral Brine A than in its diluted solution. The second increase of current can be interpreted as being due to fluctuation in which relatively mobile Ti^{+4} ions diffuse out of the crevice. In the case of highly diluted Brine A the critical Ti^{+4} concentration is rather high so that its repassivation effect can be easily changed.

An alternative explanation for the "self-healing" of an active crevice can be given from the results of Glass[9] and Diegle.[10] Glass finds that an active titanium surface in an acidic medium easily passivates if a

very small concentration of molybdate ions is added to the solution (1N H_2SO_4). This passivation occurs due to the strong bonding of polymolybdate species on the metal surface. Similarly, Diegle observed that an active titanium crevice in 1M NaCl (pH=3) repassivated when 100 ppm of Ni^{+2} ions were added to the test solution. These mechanisms of repassivation are possible in the present tests if molybdenum and nickel present in the solution from the initial dissolution of Grade-12 titanium redeposit on the active surface. Further investigations are needed on Brine A of varying dilution in order to choose between the different mechanisms of repassivation.

It is interesting to compare the current/potential behavior of Grade-12 titanium with that of Grade-2 titanium, shown in Figure 11. Firstly, the much higher corrosion current in the case of Grade-2 titanium is consistent with the physical observation of much higher corrosion. Because of the faster reaction in this case, the active dissolution stage of crevice corrosion starts during heating and there is no observable incubation period. As in the case of Grade-12 titanium, the current decreases after approximately 110 hours. However, in contrast, it is not accompanied by any increase in potential. On the contrary the crevice potential shows a further decrease. Diegle[10] and McKay and Mitton[11] have reported similar observations on Grade-2 titanium crevices in NaCl solutions. It is believed that unlike Grade-12 titanium crevices the decrease in current in Figure 11 is not due to the repassivation of anode surfaces. Presumably, the observed current goes to zero because the cathodic reaction no longer occurs on the external freely exposed cathode specimen. Instead, with increasing aggressiveness of the crevice solution the cathodic reaction moves onto the anode specimen surface. This possibility is

supported by the observation of titanium hydride in the corrosion product. In other words, as oxygen in the autoclave is consumed at the cathode surface, the importance of hydrogen reduction as a cathodic reaction increases. Griess[12] has shown earlier that the fraction of hydrogen reduction reaction can become as high as 91% in some cases. Similar observations were made by McKay and Mitten.[11] Highly acidic conditions within the crevice would further promote hydrogen evolution. Under these conditions the cathode specimen may become anodic to the creviced anode specimen to the extent that a negative current is observed and a small part of the cathode specimen is dissolved in the solution.

The previous paper[1] showed that crevice corrosion of Grade-12 titanium in neutral Brine A is facilitated if the solution is saturated with oxygen. This observation emphasizes the importance of available oxygen and oxygen reduction as the cathodic reaction. However, an approximate calculation of the total observed flow of charge in the current measurement suggests a gain in the weight of the anode specimen is typically smaller than the observed weight increase. Therefore, even for the case of Grade-12 titanium, hydrogen reduction appears to be an important cathodic reaction although hydride formation has not been observed directly. That some kind of gas evolution occurs within the Grade-12 titanium crevice is seen in Figure 6. Here the gas had detached the blister-like corrosion product from the substrate which is also covered with oxide. The picture shows a crater-like feature left behind after the breaking of the blister. The analysis of gases collected at the completion of the test also showed some hydrogen, although it is not certain if corrosion of other titanium components had contributed to this observation.

The difference between the susceptibiities of Grade-2 and Grade-12 titanium to crevice corrosion under the present conditions is striking. Whereas the much lower corrosion for Grade-12 titanium is obvious, the surface morphology of Grade-12 titanium shows (Figure 5) distinct signs of pitting, whereas that of Grade-2 titanium resembles fast dissolution.[11,22,13] According to the classical model of crevice corrosion, in the case of Grade-2 titanium, as the pH of the crevice solution decreases below a critical value the anode potential decreases into the active region. The crevice propagation stage then corresponds to the high anodic current which reaches a steady state determined by the pH, the transport of H^+ and Ti^{+3} ions out of the crevice, the titanium hydrolysis equilibria and the kinetics of the hydrogen reduction reaction.[11]

In the previous paper,[1] we discussed why pitting was observed in Grade-12 titanium. It was considered that the pitting potential was achieved locally in the β phase where there is an enrichment of alloying elements (Mo, Ni). Subsequently, the β phase was selectively dissolved locally in a manner consistent with pitting corrosion. Once a pit initiates in the β phase, it can propagate into the α phase in an autocatalytic manner. As long as the majority of the surface is not attacked, the overall metal potential stays relatively high. This is consistent with the present observations where the overall level of anode-specimen potential in the propagating stage was considerably higher in Grade-12 titanium compared to Grade-2 titanium.

5. CONCLUSIONS

Electrochemical as well as metallographic studies confirm that Grade-12 titanium and Grade-2 titanium are susceptible to crevice corrosion in Brine A

at 150°C. This brine is sufficiently aggressive to cause corrosion even if diluted one hundred times. The incubation period to initiate rapid dissolution in Grade-12 titanium within the crevice is determined to be about two-three days regardless of varying solution chemistry. This suggestes that oxygen depletion is the rate determining step for incubation time.

The crevice corrosion of Grade-12 titanium essentially follows the classical crevice corrosion mechanism. After an incubation period, crevice corrosion starts accompanied by a potential decrease and a current increase. In the later part of the propagation stage, decreasing current and increasing potential suggest that the crevice starts to repassivate, presumably due to the deposition of alloying elements on the crevice surface, or an increase in Ti^{+4} concentration. However, the observed subsurface cracking suggests that crevice corrosion may reinitiate after prolonged exposure to the test solution. In contrast, Grade-2 titanium crevice does not show any increse in potential in this stage, which can be explained by the shifting of the (hydrogen evolution) cathodic reaction to the inside of crevice rather than by repassivation.

The optical examination of the Grade-12 titanium crevice specimen consistently shows the corrosion to be isolated areas of pitting, rather than uniform dissolution. It is believed that when the crevice solution becomes highly aggressive, with decreasing pH and decreasing oxygen concentration, the β phase provides the nucleation sites for pitting.

6. REFERENCES

1. T. M. Ahn, R. Sabatini and P. Soo, "Immersion Tests and Surface Studies for Crevice Corrosion of Grade-12 Titanium in Brine Solution at 150°C," previous paper in this journal.
2. H. Jain, T. M. Ahn and P. Soo, "A Technique for Characterizing Crevice Corrosion Under Hydrothermal Conditions," International Symposium of Laboratory Corrosion Tests and Standards, Bal Harbour, Florida, November 1983. Also to be published as a Symposium Volume by ASTM.
3. P. F. Taylor and C. A. Caramihas, "Crevice Corrosion in High-Temperature Aqueous Systems Potential/pH Measurements in Alloy 600 Crevices at 288°C," J. Electrochemical Society 129, p. 2458 (1982).
4. D. B. Stewart and R. W. Potter "Application of Physical Chemistry of Fluids in Rock Salt at Elevated Temperature and Pressure to Repositories for Radioactive Wastes," in Scientific Basis for Nuclear Waste Management, Vol. 1, p. 297, G. J. McCarthy, Editor, Plenum Press, New York, 1979.
5. Long-Term Performance of Materials Used for High Level Waste Packaging, NUREG/CR-3405, Vol. 1, Battelle Columbus Laboratories. Compiled by D. Stahl and N. E. Miller, July 1983.
6. Titanium Information Bulletin, IMI-5020/220, IMI Titanium, Birmingham, England, 1976.
7. J. W. Oldfield and W. H. Sutton, "Crevice Corrosion of Stainless Steels," British Corrosion J., Vol. 13, 104 (1978).
8. E. J. Kelly, "Anodic Dissolution and Repassivation of Titanium in Acidic Media. III. Chloride Solutions," J. Electrochemical Society, Vol. 126, 2065 (1979).

9. R. S. Glass, "Passivation of Titanium by Molybdate Ion," Extended Abstracts, Vol. 83-2, Abstract No. 153, Electrochemical Society Meeting, Washington, D. C., 1983.

10. R. B. Diegle, "New Crevice Corrosion Test Cell," Materials Performance, NACE, p. 43, March 1982.

11. P. McKay and D. B. Mitton, "An Electrochemical Investigation of Localized Corrosion on Titanium in Chloride Environments." Paper to be published.

12. J. C. Griess, "Crevice Corrosion of Titanium in Aqueous Salt Solutions," Corrosion, NACE, Vol. 24(4), 96 (1968).

13. B. S. Lee, T. M. Ahn and P. Soo, "Crevice Corrosion of Titanium in a Brine Solution," Extended Abstracts Vol. 82-2, Electrochemical Society Meeting, Detroit, Michigan, October 1982.

ACKNOWLEDGEMENT

This work was performed under the auspices of the Nuclear Regulatory Commission (NRC). The authors acknowledge the program coordination by Dr. M. McNeil of the NRC. Also they acknowledge helpful suggestions made by Dr. D. Taylor of General Electric Company and Dr. R. Diegle of Sandia National Laboratories in the initial design of the crevice corrosion cell.

Brookhaven National Laboratory Report

BNL-NUREG-34792 (1984)

A MODEL FOR THE INITIATION OF CREVICE CORROSION IN GRADE-12 TITANIUM IN A BRINE SOLUTION*

T. M. Ahn

Department of Nuclear Energy
Brookhaven National Laboratory
Upton, New York, 11973

Key Description: Titanium, Crevice Corrosion Model, Diffusion, Migration

ABSTRACT

A model is developed for the initiation of crevice corrosion of Grade-12 titanium in high temperature brine. It is based on experimental results from immersion tests, surface analyses and electrochemical measurements. During crevice corrosion, the anode potential initially increases due to the growth of a corrosion barrier oxide which consumes the oxygen inside the crevice, until the maximum potential is reached. At the maximum potential the barrier oxide stops growing, and the following potential drops are governed by the solution chemistry change within the crevice. The potential changes associated with the solution chemistry include (1) a potential drop caused by an oxygen concentration change (2) an ohmic potential drop (3) a potential rise due to pH changes and (4) a potential rise due to excess proton generation. For the growth of oxide, a simple mass balance gives the potential rise as the oxide thickness is increased. Simplified diffusion equations for the concentrations of oxygen, proton and anions are used to estimate the chemistry change inside the crevice. Diffusion caused by the concentration gradient and potential field within the crevice are considered. For the chemistry change, the potential is calculated using the Nernst equation. Potential changes are compared to experimental values. The comparison allows an estimate to be made of the concentration gradient distance. The final equations attained are used to draw domains for crevice corrosion initiation on a temperature/anion concentration diagram. The calculated domains are consistent with measured domains available in the literature. Also the equations developed provide a technique for estimating the solution chemistry inside the crevice as a function of time and the final crevice chemistry at equilibrium. Since the calculated (limiting) crevice chemistry is very aggressive, crevice corrosion is inevitable over a wide range of conditions.

FIGURES

TABLES

1. INTRODUCTION

As shown in the previous two papers,[1,2] immersion tests, surface analyses and electrochemical studies have shown that macroscopic concentration cell formation is responsible for Grade-12 titanium crevice corrosion in a simulated rock salt brine at 150°C. Cell formation is accompanied by oxygen depletion, a potential drop, anion accumulation and acidification inside the crevice. This leads to pit initiation. To quantify the crevice corrosion process, surface films have been analyzed and the anode and cathode reactions have been studied using a specially-designed cell in which the two electrodes are physically separated. The anode potential, current flow from cathode to anode and pH inside the crevice have been monitored. In this paper, we present a simplified model to explain the results of the surface analyses and the electrochemical measurements.

Among the five models available to explain crevice corrosion in the literature,[3-7] two comprehensive models have been chosen for study: (1) an electrochemical/hydrodynamic model[6] considering sample geometry effects and (2) an electrochemical model with a minor modification for hydrodynamic effects.[4] Our experimental design may be interpreted better by the latter model[4] for the following reasons: (1) the sample size is large enough and the dissolution rates are fast enough to minimize diffusion effects i.e., sample geometry effects, (2) the crevices used in the present work are obtained by tightly joining two coupons. Since the crevice gap will not be constant on a local scale because of surface imperfections, the model with sample geometry effects[6] is less applicable. Also, the former model has only a numerical solution, so it is difficult to visualize the functional dependence of mass

balance and to extrapolate behavior to extended times. On the other hand, the latter model does not consider hydrodynamic mass balance quantitatively and excludes surface characterization results. To resolve these shortcomings, we present a simplified model based on our experimental observations.

2. UNDERLYING MECHANISMS AND BASIC ASSUMPTIONS

The anode potential increases continuously during the growth of a barrier oxide (anatase form of TiO_2) until the maximum potential is reached. The relation of the oxide thickness and the electrode potential is linear.[8,9] After the maximum potential is reached, the barrier oxide stops growing and the following potential drops are governed mainly by solution chemistry changes in the crevice. The solution chemistry changes from the initial state beginning by the consumption of oxygen inside the crevice and by the subsequent anode-cathode separation stage which causes accumulation of protons and anions inside the crevice. The potential change caused by the solution chemistry modification is obtained by considering (1) a potential drop caused by an oxygen concentration change,[10,11] (2) an ohmic potential drop,[5,12] (3) a potential rise due to pH changes,[11] and (4) a potential rise due to excess proton generation.[13] Because of the solution chemistry change, a pitting environment forms. Contribution (2) is approximately negated by contribution (3) based on calculations for estimating the ohmic potential.[11] Also, contribution (4) is, typically, negligible because of the conservation of charge neutrality.[13] Therefore, after the maximum potential is readied, the effects of oxygen depletion are dominant and complete oxygen depletion is an important prerequisite for pit initiation since a pit initiates when the potential becomes low while the oxide thickness remains constant.[14] We assume

that this oxygen depletion stage is the critical condition for the initiation of crevice corrosion. In the preceding paper, the initiation times for varying proton and anion concentrations are shown to be similar, supporting our assumption that oxygen depletion is the critical condition for the initiation of crevice corrosion. We exclude the consideration of the complicated kinetic process of monolayer formation at the Flade potential in pits. This is a conservative criterion for the initiation condition.

During mass transport, protons are generated in the crevice by the anode-cathode separation process. Diffusion and field-enhanced diffusion (migration) terms decrease the proton concentration. Oxygen is consumed but is still supplied by diffusion from outside the crevice. Anions migrate into the crevice to neutralize the protons generated, while the accumulated anions are moved out by diffusion.

Instead of adopting partial differential equations and boundary conditions for mass balance calculations, we use the effective concentration gradient distance, δ, which allows us to describe the diffusion equation in simple terms. We use a linear concentration or potential gradient across this value δ. This is a valid assumption when δ is very small compared to the sample size. In the calculation of potential using the Nernst equation, the concentration term is used instead of the activity. For migration calculations, the potential term is obtained from the anion concentration on the basis of assumptions used by Vermilyea.[12] Our major consideration concerns the proton and chloride ions since they are the major ions present. Other types of anion are in small concentrations and their diffusivities are slower or, at most,

close to that for chloride ions.[15] Therefore, chloride and proton concentrations are considered to determine the passivity breakdown condition.

3. FORMULATION OF EQUATIONS AND COMPARISON TO EXPERIMENTAL RESULTS

The anode potential rise during the growth of barrier oxide is given by the following mass balance relationship:

$$V(\text{oxide}) = V_i + I_p\ t\ M/(c\ \rho\ F) \qquad (1)$$

where ρ is the density of the anatase form of TiO_2, c is a proportionality constant (8,9), I_p is the passive current estimated from the maximum potential observed, t is the time, M is the molecular weight of TiO_2, F is the Faraday constant and V_i is the initial potential. We have used the initial value of potential as that measured at the time when appreciable current flow (~1 μA range) is observed. The potential drop due to the oxygen concentration change may be approximated by the Nernst equation:[10,11]

$$V(O_2) = V_i + \frac{RT}{F} \ln \left(\frac{C(O_2)}{C_i(O_2)}\right) \qquad (2)$$

where $C_i(O_2)$ is the initial oxygen concentration and $C(O_2)$ is the oxygen concentration at time t. $C(O_2)$ is obtained by a simplified diffusion equation:

$$C(O_2) = C_i(O_2) - \frac{2\ I_p t}{H\ F} + \frac{2\ D_{O_2} + t}{x\ \delta} [C_i(O_2) - C(O_2)] \qquad (3)$$

where x is the crevice depth, H is the crevice gap size, δ is the effective length of the oxygen concentration gradient within the crevice, and D_{O_2} is

the oxygen diffusivity. The second term represents oxygen concentration consumed and the third term represents oxygen concentration by diffusion inflow. Upon separation of the anodic and cathodic areas, a current, I, flows from the cathode to the anode resulting in the accumulation of protons, and in the migration of chloride ions to the crevice. The accumulated concentrations of protons $C(H^+)$ and chloride ions $C(Cl^-)$ are given by the following mass balance equations:

$$C(H^+) = C_i(H^+) + \frac{2\ I\ t}{F\ H} - \frac{2\ D_{H^+}\ t}{x\ \delta}\ [C(H^+)-C_i(H^+)]$$

$$- \frac{2\ D_{H^+}\ t\ C(H^+)}{x\ \delta}\ \ln\ (\frac{C(H^+)}{C_i(H^+)}) \qquad (4)$$

$$C(Cl^-) = C_i(Cl^-) - \frac{2\ D_{Cl^-}\ t}{x\ \delta}\ [C(Cl^-)-C_i(Cl^-)]$$

$$+ \frac{2\ D_{Cl^-}\ t\ C_i(Cl^-)}{x\ \delta}\ \ln\ [\frac{C(H^+)}{C_i(H^+)}] \qquad (5)$$

where $C_i(H^+)$ and $C_i(Cl^-)$ are initial concentrations of proton and chloride ion, respectively, and D_{H^+} and D_{Cl^-} are diffusivities of the proton and the chloride ions, respectively. The above two equations have diffusion terms arising from the concentration gradient and from field-enhanced diffusion (migration). The field potential is approximated using the proton concentration.[12] From these two equations, the ohmic potential drop may be given by:[5,12]

$$V(\text{ohmic}) = V_i + \frac{RT}{F} \ln \left[\frac{C_i(HCl)}{C(HCl)}\right] \qquad (6)$$

where $C_i(HCl)$ and $C(HCl)$ are HCl concentrations at t=0 and t, respectively. The potential change due to the pH decrease is approximately the negative value of Equation (6). Therefore, the net effect is from the oxygen concentration [Equation (2)].

The best fit to our experimental data (neutral Brine A) is shown in Figure 1 for δ = 0.3 cm (effective distance of concentration gradient), Ip = 7.6×10^{-10} amp/cm^2 (passive current with oxygen reduction), c = 2.5×10^{-7} cm/volt[9,10] (a proportionality constant between oxide thickness and electrode potential), crevice depth = 2.54 cm, crevice gap = 2 μm, an oxygen diffusivity (cm^2/sec) of 0.0821 exp(-2440/T),[16] a proton diffusivity (cm^2/sec) of 0.02838 exp (-1700/T),[16] chloride diffusivity (cm^2/sec) of 0.0508 exp(-2327/T),[16] and an anatase density of 3.84 gm/cc.[17] Very little change occurs in Figure 1 with a current variation from 0.24 to 10 μA/cm^2, because the main potential drop arises from oxygen effects. Figure 2 shows the concentration profiles in the crevice at various testing times for a current density of 10 μA/cm^2. Because the brine solution has a near saturated Cl^- ion concentration, the calculated large value indicates some types of precipitates which may form. Also, the low pH level indicates that the actual pH at higher temperatures is much lower than that measured at room temperature (experimental values vary from 2.8 to 4.5). Two curves for oxygen concentrations are shown for different crevice heights. As expected, an increased crevice gap size delays the oxygen depletion time significantly. This is also true for increasing crevice area.

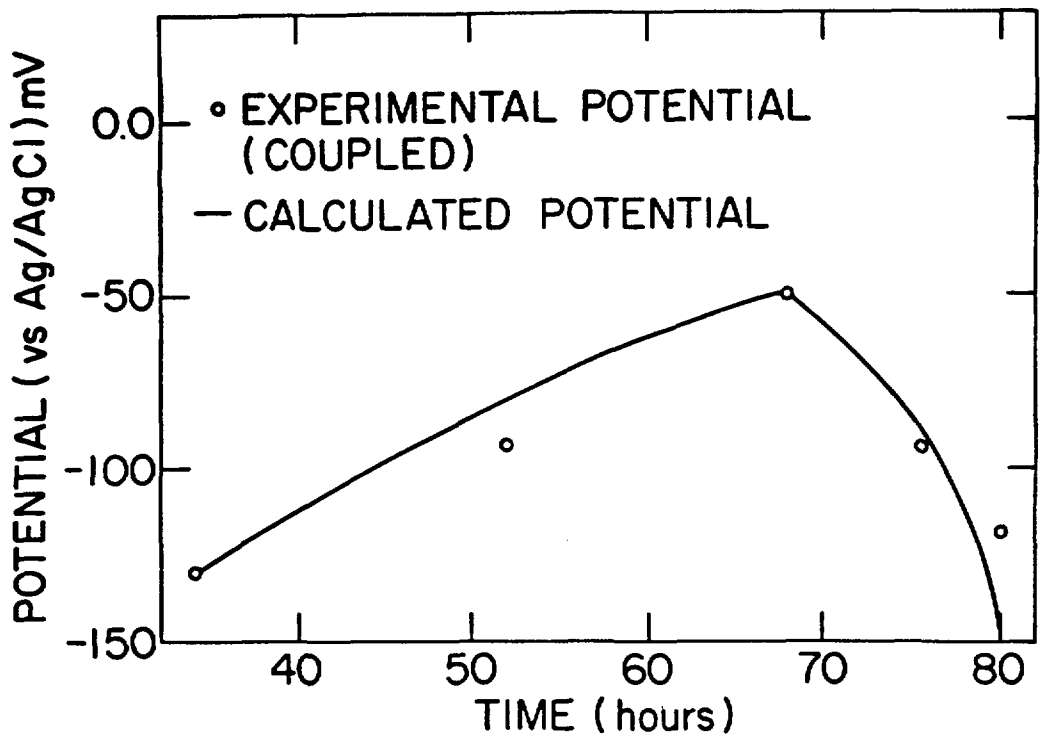

Figure 1. Experimental potential (open circles) and "fitted" potential (solid line) of coupled Grade-12 titanium crevices in aerated neutral brine at 150°C.

Data fitting was not performed for the results obtained in the solution varying concentrations. During the initiation period, the essential features for all cases were identical within the scatter of the experimental values. The detailed comparisons are out of the scope of present works.

The solution within a crevice will tend to have a limiting composition as the corrosion time approaches infinity. From the predictive equations [Equations (3), (4) and (5)] the limiting concentration is obtained by dividing each term by time t and letting time approach infinity. Calculation shows that there is no limiting pH and oxygen concentration, and these parameters can theoretically fall to extremely low values within the crevice. Table 1 shows the computed limiting values of Cl^- concentration within the crevice for assumed values of pH. Note that these Cl^- concentration levels are in excess of 10^6 ppm which is not physically possible. However, the analytical approach serves to show that extremely high levels of chloride will accumulate with time.

Table 1. Calculated limiting chloride concentrations at infinite time in the crevice of Grade-12 titanium in aerated neutral Brine A at 150°C.

Limiting pH	-1	0	1	2	3
Limiting Cl^- Concentration (ppm)	3,690,560	3,279,590	2,815,420	2,377,850	1,940,280

The initial Cl^- concentration is 190,000 ppm. A Cl^- concentration of more than 10^6 ppm implies that there is no practical limitation on chloride ion accumulation as time progresses.

To study the effects of initial chloride concentration and temperature, a calculation was performed based on the above discussion. With pH = -1.19 in Figure 2 and the critical value of chloride ion concentration for passivity breakdown taken to be 190,000 ppm (near saturation of brine with chloride ions), a map is drawn in the space of temperature and the initial chloride concentration $C_i(Cl^-)$ necessary to attain the critical concentration at various times. A calculation was performed using Equation (5) by setting $C(Cl^-)$ = 190,000 ppm and pH = -1.19 for $C(H^+)$. As expected, smaller amounts of initial chloride ions are needed at higher temperatures for the initiation of crevice corrosion. Such domains have been experimentally determined in unalloyed Ti and Ti-Pd alloys exposed to dilute sodium chloride solutions.[18] Therefore, our simple formulation is promising. Further, this calculation permits the extrapolation to long term behavior. Inside the unshaded area of Figure 3, crevice corrosion occurs while the hatched area shows immunity to crevice corrosion. The boundary between the two domains is affected by the corrosion time with the domain for crevice corrosion becoming larger as corrosion times are increased. At infinite corrosion time, the boundary becomes a straight line designated by C_{th}, below which crevice corrosion does not occur even at infinite time.

Note that the curves in Figure 3 have been calculated on the basis of a corrosion current which is independent of test temperature. When the temperature dependence of the current is considered, the curves in this figure depend more strongly on the chloride concentration. Also, the model developed shows that there will be a temperature limit, T_{th}, below which mass flow in the corrosion system ceases. Since the calculated T_{th} is lower than the

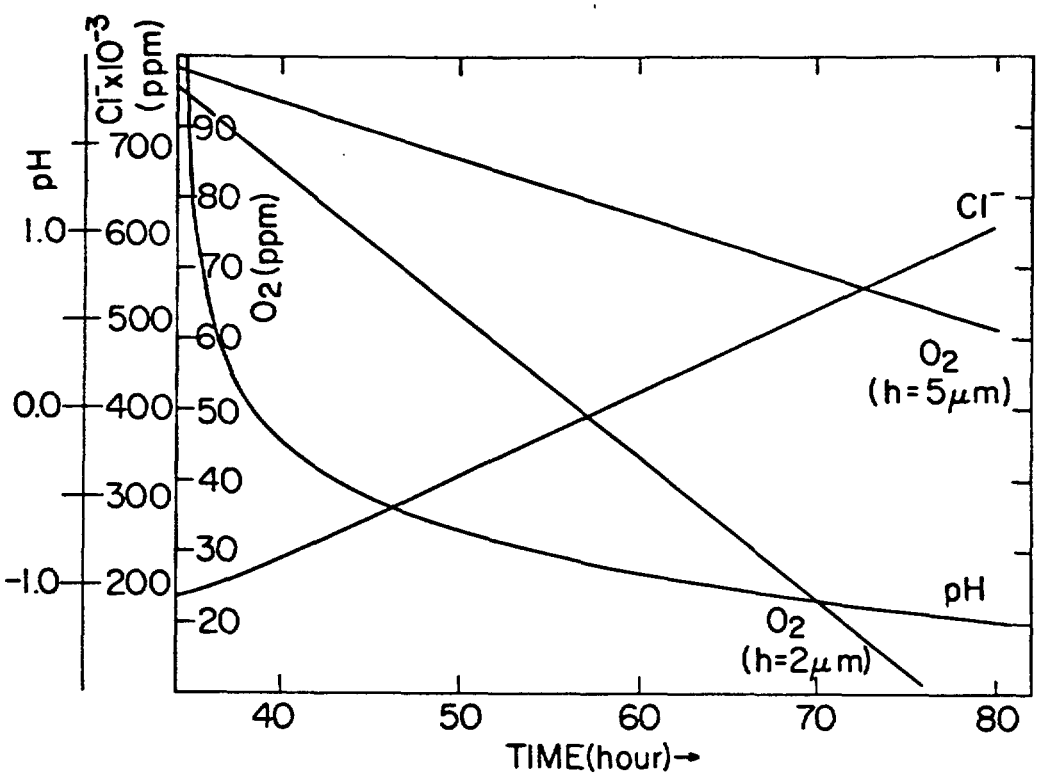

Figure 2. The calculated concentration profiles in the crevice at various testing times for a current density of 10 $\mu A/cm^2$.

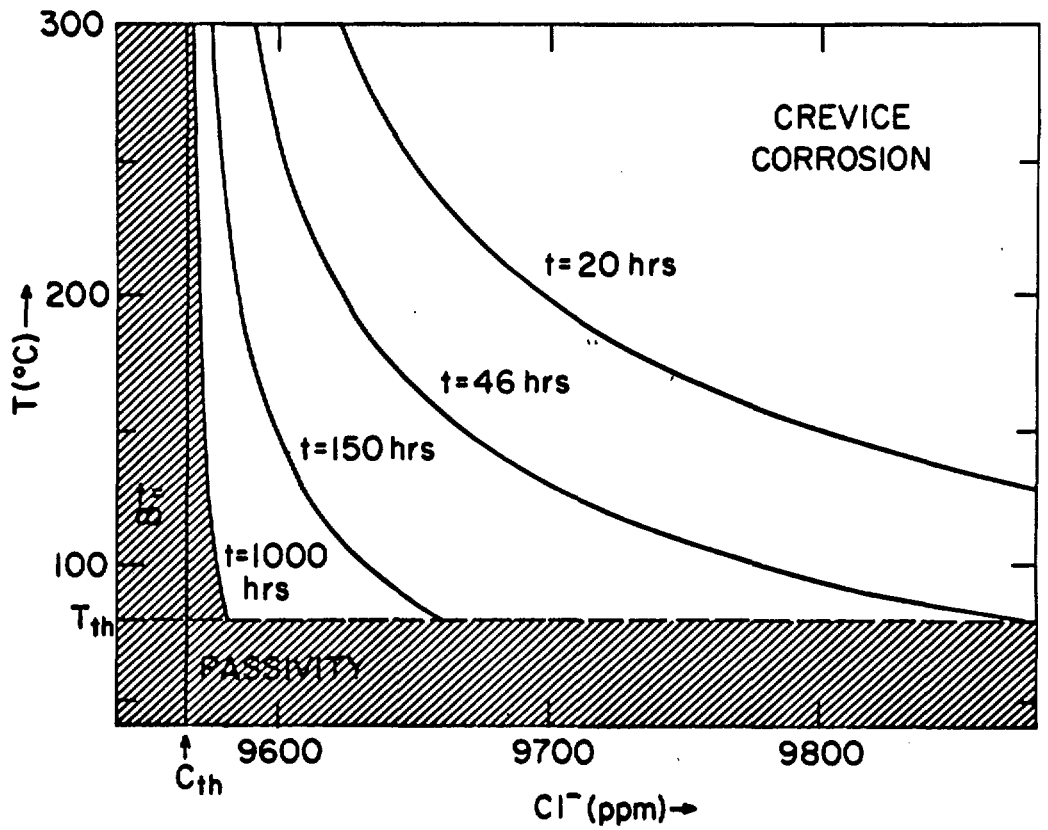

Figure 3. Immunity domains for crevice corrosion at various service times for Grade-12 titanium in a simulated rock salt brine. The critical anion concentration assumed for passivity breakdown is 190,000 ppm.

freezing point of the test solution, it does not have a significant meaning at these low temperatures.

4. DISCUSSION

In the above crevice corrosion analysis, we have used a linear variation of the concentration gradient introducing an adjustable parameter δ (effective concentration gradient distance). Severe crevice corrosion at the edges of test specimens supports the assumption that δ is very small compared to the specimen size. This is also predicted in our calculations. We have used concentration instead of activity in the calculation of potential. The present experiments do not provide activity coefficients for various ions at high temperatures. However, since most of the activity coefficients are incorporated in logarithmic terms for the potential calculation, the adjustable parameter δ will not significantly change with variations in the activity coefficient.

We have not calculated the pH necessary for breaking down of passivity as a function of temperature mainly because we do not have a value for I in Equation (4) as a function of temperature and pH. I values are known to be a strong function of temperature and pH. Nevertheless, we could see that the lower pH is necessary at lower temperature qualitatively when the dependence of I on temperature and pH is stronger than the dependence of diffusivity on temperature. This was observed in the experiment also (Figure 4).[18] When the I values dependent on temperature are used in the calculation, the initial chloride concentration necessary for passivity breakdown will vary more strongly with temperature, as observed experimentally.

We have approximated the potential term for migration with the concentration variation. Strictly speaking, this assumption is only valid for dilute

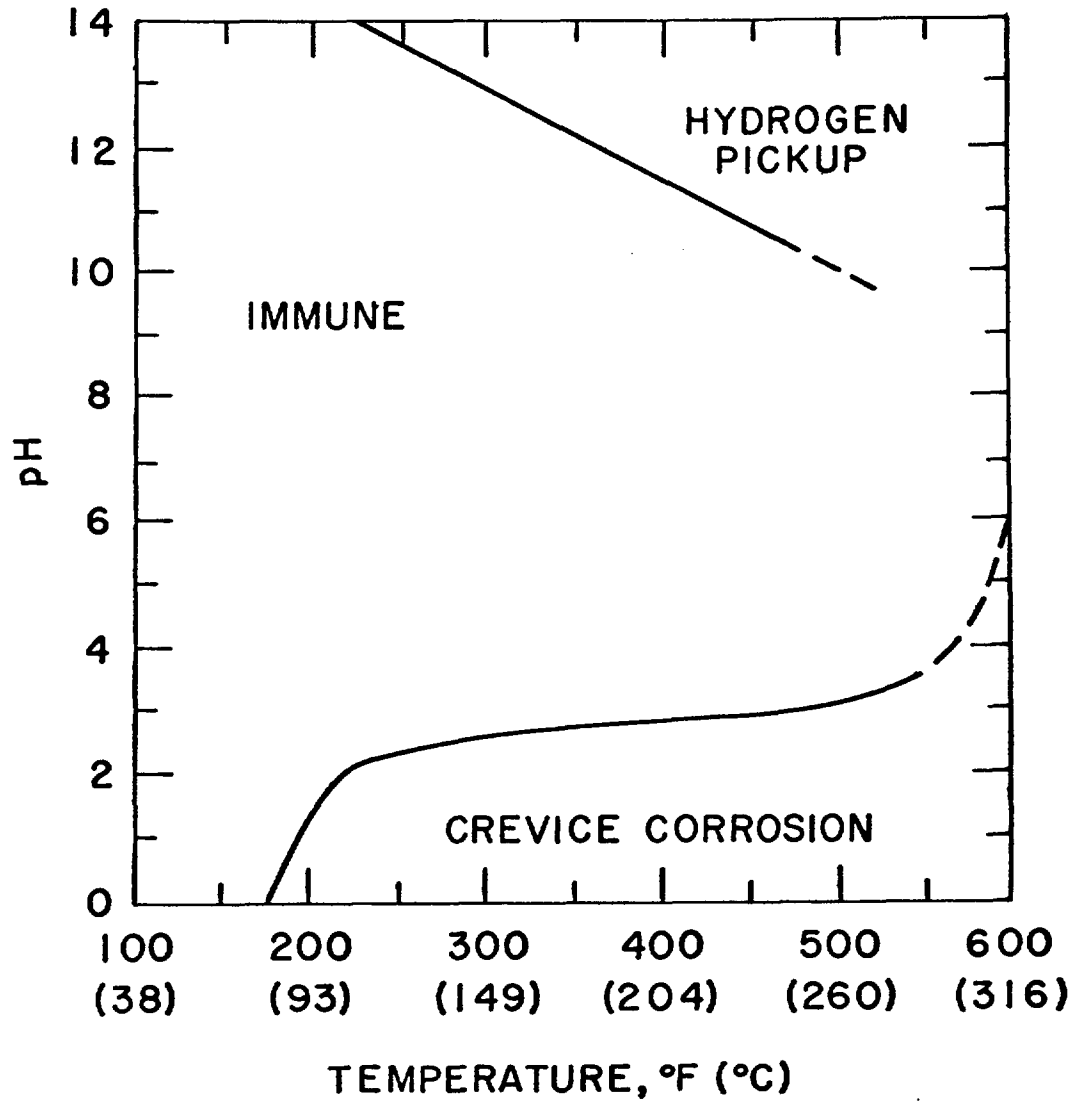

Figure 4. Immunity domains in temperature and pH necessary for passivity breakdown for CP titanium.[18]

solution. However, since we were concerned only with proton concentration, this assumption should be valid even though we have high anion concentrations.

Critical anion concentration for passivity breakdown has been assumed to be the near saturated concentration value. In diluted solutions, it may be possible that the critical anion concentration is smaller than the near saturated concentration. In this case, the initial anion concentration necesary for passivity will be reduced according to Equation (5).

5. CONCLUSIONS

A mass balance model was developed for the initiation of crevice corrosion. The basic process is the classical crevice corrosion mechanism obtained from immersion tests, surface analyses and electrochemical measurements. Initially the crevice potential rises because of the growth of a corrosion barrier oxide which consumes oxygen inside the crevice. After the maximum potential is reached, the barrier oxide stops growing and the following potential drop is governed by the solution chemistry change in the crevice. The potential drop resulting from oxygen depletion is the major source of potential change. A simple mass balance equation gives the potential rise as the oxide thickness is later increased. Simplified diffusion equations for oxygen, protons and anions were used to estimate the chemistry change inside the crevice. The potential drop was calculated using thermodynamic approximations. The calculated value was compared to an experimental value in order to estimate unknown parameters. The final equation was used to draw a map for crevice corrosion initiation in a temperature/anion concentration diagram. The calculated domains are consistent with experimental values. The equations also allow the chemistry inside the crevice to be estimated as a function of time.

6. REFERENCES

1. T. M. Ahn, R. Sabatini and P. Soo, "Immersion Tests and Surface Studies for the Crevice Corrosion of Grade-12 Titanium in a Brine Solution at 150°C." Preceding first paper.
2. H. Jain, T. M. Ahn and P. Soo, "An Electrochemical Study of Crevice Corrosion of Grade-12 Titanium in a Brine Solution." Preceding second paper.
3. J. L. Crolet and J. M. Defranoux, "Calculation of the Incubation Time of Crevice Corrosion in Stainless Steels," Corrosion Science 13, 575 (1973).
4. J. W. Oldfield and W. H. Sutton, "Crevice Corrosion of Stainless Steels," British Corrosion J. 13, 13 (1978).
5. ORNL-TM-4099, "Kinetics of Initiation of Crevice Corrosion of Titanium, Water Research Program Biannual Progress Report for the Period of March 15, 1966 to March 15, 1968," F. A. Posey and D. V. Subrahmanyam, Oak Ridge National Laboratory, 1973.
6. D. W. Siitari and R. C. Alkire, "Initiation of Crevice Corrosion," J. Electrochemical Society 129, 482 (1982).
7. B. Vincentini, D. Sinigaglia and G. Taccani, "Crevice Corrosion: Calculation of the Voltage and Current Distribution Along the Crevice," Werkstoffe and Korrosion 22, 916 (1971).
8. T. R. Beck, "Initial Oxide Growth Rate on Newly Generated Surfaces," J. Electrochemical Society 129, 2501 (1983).
9. J. F. McAleer and L. M. Peter, "Instability of Anodic Oxide Films on Titanium," J. Electrochemical Society 129, 1252 (1982).
10. H. H. Uhlig, Corrosion and Corrosion Control, John Wiley and Sons, Inc., p. 11, p. 26, 1971.

11. J. O'M. Bockris and D. M. Drazic, Electrochemical Science, Barnes and Noble Books, New York, p. 141, 1972.

12. D. A. Vermilyea and C. S. Tedmon, Jr., "A Simple Crevice Corrosion Theory," J. Electrochemical Society 117, 437 (1970).

13. J. Newman, "Mass Transport and Potential Distribution in the Geometries of Localized Corrosion," in Localized Corrosion, Edited by R. W. Staehle, B. F. Brown, J. Kruger and A. Agrawal, NACE-3, 1974.

14. K. Shimogori, H. Sato and H. Tomari, "Crevice Corrosion of Titanium in NaCl Solutions in the Temperature Range 100 to 250 Degree C." J. of Japan Institute of Metals, 42(b), 1978.

15. Y. H. Li and S. Gregory, "Diffusion of Ions in Sea Water and in Deep-Sea Sediments," Geochimica et Cosmochimica Acta 38, 703 (1974).

16. A. Lerman, Geochemical Processes Water and Sediment Environments, John Wiley and Sons, Inc., p. 103, 1979.

17. Handbook of Chemistry and Physics, CRC Press, 62nd Edition, 1981-1982.

18. "Titanium Heat Exchangers for Service in Seawater, Brine, and Other Aqueous Environments," Titanium Information Bulletin from IMI, Birmingham, England, 1979.

ACKNOWLEDGEMENT

This work was performed under the auspices of the Nuclear Regulatory Commission (NRC). The author acknowledges program coordination by Dr. M. McNeil of the NRC. Also he acknowledges helpful discussions with Dr. P. Soo of Brookhaven National Laboratory.